QUANTUM ELECTRODYNAMICS OF RESONANCE ENERGY TRANSFER

GEDIMINAS JUZELIŪNAS

Institute of Theoretical Physics and Astronomy, Vilnius, Lithuania

DAVID L. ANDREWS

School of Chemical Sciences, University of East Anglia, Norwich, England

CONTENTS

Advances in Chemical Physics, Volume 112. Edited by I. Prigogine and Stuart A. Rice
ISBN 0-471-38002-4.

I. INTRODUCTION

More than a half century has elapsed (at the time of writing) since the first pioneering attempts by Fermi [1], Heitler and Ma [2], and Hamilton [3] (following a related study by Kikuchi [4]) to address the methods of quantum electrodynamics (QED) to resonance energy transfer (ET), a process in which the excitation energy of an atom, molecule, or other species D (to be referred to as the *donor*) is transferred to another entity A (the acceptor) separated from it by some distance R. The early QED theories of this process [1–3] concentrated on the radiative ET principally manifest at far-zone distances $R \gg \lambda\!\!\!^{-}$, where $\lambda\!\!\!^{-} = \lambda/2\pi$ and λ is the wavelength associated with the photon conveying the energy from D to A. In these early works it was shown that the transfer probability properly behaves as R^{-2}. Furthermore there was a relativistic time lag of R/c associated with propagation of the photon to the acceptor; in other words, the process satisfies the basic requirements of causality. This much is in agreement with what is expected from classical electrodynamics. Radiative transfer of energy can take place over various distances, including those of cosmic scale (in the case of energy coming from distant stars). At the other extreme, however, radiative energy transport can also occur between donor and acceptor sites within a single object (as long as $R \gg \lambda\!\!\!^{-}$); in particular, it is a mechanism leading to the re-absorption of emitted photons in optically thick samples [5,6].

Almost at the same time as the first work on the QED of radiative ET [1–3], another radiationless mechanism was suggested by Perrin [7], Förster [8], Dexter [9] and Galanin [10] to deal with near-zone ($R \ll \lambda\!\!\!^{-}$) energy transport. This mechanism treats the process as one induced by the instantaneous (Coulomb) interaction between the transfer species D and A. As a result, Förster arrived at an R^{-6} dependence for the transfer rate in the case where the process is governed by dipole-dipole coupling between the donor and acceptor [8]. Radiationless ET takes place in a wide variety of condensed systems, such as concentrated solutions [6,11] and, most importantly, in photosynthetic light-harvesting antennas [12–14]. Through its contextual significance in advancing both the fundamental understanding of biological photosynthesis, and informing strategies for synthetic mimicry of the latter, the process has attracted a greatly increasing interest in recent years.

In the 1960s Avery [15] and Gomberoff and Power [16] attempted to use the QED approach to generalize the Förster theory of short-range (radiationless) ET [8,10,11] to arbitrary transfer distances. Such a unified approach to radiationless and radiative ET, in which the process is considered to be mediated by intermolecular propagation of a virtual photon, has received a considerable boost in the 1980s [17–22] and 1990s [22–32]. Through these studies it has been demonstrated [15,16,18,19,21,27,31] that the unified

mechanism reproduces the Förster R^{-6} dependence of the transfer rates in the near zone — whereas in the far zone, resonance ET equates to emission of a photon by a donor molecule and subsequent recapture of the photon by an acceptor. It has also been shown [33] how the unified theory may be extended to include the effects of very short-range nondipolar coupling, associated with localized molecular-orbital interactions through the involvement of charge-transfer configurations. This approach offers a seamless extension of the Förster theory to regions of strong orbital overlap, where excitation transfers as in the Dexter exchange interaction [9]. In other developments [25,28,30,34–38], the time evolution of the transfer dynamics has been explicitly considered within the framework of the unified theory, addressing in detail the transfer dynamics beyond the rate regime. Among other issues, an intricate problem of causality in ET (initially raised by Fermi [1]) has been reexamined [25,39–52]. Another related problem concerns collective emission (super- and subradiance) by two atoms interacting via the resonance dipole–dipole coupling [34,35,53–58] a phenomenon finding an interest in laser cooling [59,60]. It is also worth mentioning the spontaneous emission by a molecule near a metal surface [61–65]. Such a process might be considered in certain respects as the resonance ET between the molecule and its image, although a more rigorous analysis of the phenomenon is to be based on the coupling of the excited molecule to surface plasmons [64,65]. It is noteworthy that the resonance ET belongs to a wider class of bimolecular photophysical processes [66,67] mediated by a virtual photon. Other bimolecular processes, such as the (third-order) single-photon cooperative absorption [68–70] or emission [71], involve creation or annihilation of real photons as well.

Another important raft of issues relates to the incorporation within the unified theory of the effects of the surrounding medium. Although a handful of sporadic attempts to accommodate medium effects in excitation transfer appeared previously [15,22,24], it was the case until quite recently that most QED theories totally ignored the influence of such effects. The 1989 treatment by Craig and Thirunamachandran [22], incorporating effects of a third molecule in the resonance ET between a selected pair of molecules, led to a new discussion of the way to include dielectric characteristics. It was suggested from macroscopic arguments that the vacuum dielectric permittivity ε_0 entering the rate of excitation transfer in vacuo should be replaced by its medium counterpart ε to represent the screening. Nevertheless, in using this prescriptive approach, other important medium effects, such as local fields, energy losses due to the absorbing medium, and influences on the character of the transfer rates in passing from the near zone to the far zone, were not considered.

More recently a QED theory has been developed [27,28,31] that systematically deals with these issues. A fully second-quantized formalism has been adopted to treat the effects of the molecular medium at the microscopic level.

In contrast to conventional QED theories for the resonance ET between a pair of species in vacuum [15–26], in which the process is considered to be mediated by the intermolecular propagation of virtual photons, the new theory [27,28,31] has been formulated by invoking the concept of bath polaritons ("medium-dressed photons") mediating the ET. To this end, the approach has some analogies with related work [72] on intermolecular forces and superradiance, in which a lossless medium was modeled by an ensemble of two-level species. The theory developed in Refs. 27 and, 28 (as well as subsequent work [31,73]) accommodates an arbitrary number of excited states of electronic, vibrational, and other origin for each molecule of the medium. This includes, in particular, a case of special interest, where the excited-state spectrum of the molecules is sufficiently dense and smooth for it to be treated as a quasicontinuum. In such absorbing regions of the spectum, the exponential (Beer law) decay factor emerges in the microscopically derived rates for ET between a selected pair of species (pair-transfer rates). This feature also solves the problem of potentially infinite rates of the resonance ET in the ensemble, due to the far-zone inverse-square law, featured in the pair-transfer rates [27,28,31] (see Section V for more detail). Furthermore, the pair rates contain other refractive modifications, such as the local field factors.

Other recent studies have analyzed the resonance coupling between molecules situated in photonic bandgap crystals [71,74–78], in plasma media [79], between metal or dielectric plates [80,81], in dielectric microparticles (Mie particles) [82–86], and in other cavities [87,88]. Such systems can exhibit an optical response that fails to support the propagation of certain optical frequencies.* The spontaneous emission is inhibited within the bandgaps of the photon spectra [71,89–93] and no radiative limit exists for the resonance ET. Nevertheless, it has been demonstrated that ET can take place quite efficiently between species separated by distances up to those comparable with the wavelength of light or even somewhat larger [71]. This might serve as an alternative relaxation channel for excited atoms or molecules, the transition frequencies of which are tuned to the photonic bandgap.

It is the purpose of this chapter to review the QED approach to energy transfer taking place both in the free space (electromagnetic vacuum) and in media. The plan in the following sections is to work as follows:

- In Section II we define the basic concepts of quantum electrodynamics of resonance energy transfer, subsequently providing the derivation of the transition matrix element for the ET between a pair of chromophores

* On the other hand, the photon spectra might also exhibit singularities (such as Mie resonances [81–86]) at some other frequencies.

separated at an arbitrary distance R. At this stage the medium surrounding the transfer species, is not explicitly specified.

- The second step (Section III) is to calculate the tensor for the resonance dipole–dipole coupling between a pair of molecules (or atoms) in the electromagnetic vacuum, in a photonic bandgap crystal, as well as in a homogeneous dielectric medium. The latter dielectric medium is considered to be comprised of discrete atoms or molecules, so that the analysis is free of phenomenological assumptions.
- The subsequent analysis concentrates on the ET in the dielectric medium. In Section IV the energy-level structure is included for each donor and acceptor. Accordingly, the transfer rate is represented in terms of the overlap integral between the donor fluorescence and the acceptor absorption spectra (Section IV.A), establishing a firm connection with both the Förster R^{-6} radiationless result and the radiative limit. The transfer rate contains the required refractive modifications, including, inter alia, the local field factors. The consideration of the range dependence of the fluorescence depolarisation (Section IV.B) illustrates the approach.
- The next element (Section V) is to analyze the total rate of decay of an initially excited molecule, due to the ET to the surrounding medium. The contribution associated with the ET to the far-zone species is then identified as the rate of spontaneous emission in the absorbing medium. The emission rate contains the local field factors that support the previous phenomenological results obtained using other methods.
- Section VI analyses in detail the transfer dynamics for a pair of species in the dielectric medium. The section not only extends consideration beyond the rate description, but also reexamines conditions for that regime itself. That leads to incorporation of the shifts in energy for both the ground and excited states of the transfer species, due to the interaction of these species with the molecules belonging to the medium and also with each other. Attention is then focused on situations that do not fit into the rate regime, and where different dynamical aspects are apparent. The problem of causality in the ET is also here discussed.
- Finally, the concluding section, Section VII, summarizes the material presented in this chapter.

II. GENERAL FORMULATION

A. Hamiltonian

The framework within which the unified theory naturally emerges is nonrelativistic (molecular) QED [94–96], best implemented in its multipolar (Power–Zienau–Woolley) formulation [96–98]. In such a multipolar

formulation, the Coulomb interaction between electrically neutral molecules (or atoms) completely cancels, and it is the coupling of the molecules with the transverse photons that is responsible not only for molecular absorption and emission but also for the intermolecular coupling via the exchange of virtual photons. Consequently, retardation is naturally accommodated, reflecting the finite speed of signal propagation. It is such retardation features, for example, that are responsible for modifying at mesoscopic distances the inverse sixth-power distance dependence of the London potential (the attractive part of the 6–12 Lennard-Jones potential) to the correct and experimentally verified form given by the Casimir–Polder formula — in which the asymptotic behavior at large distances proves to be of inverse seventh power form [96,99].

In the multipolar formulation of QED, the Hamiltonian for the system can generally be written as

$$H = H_{\text{rad}} + \sum_X H_{\text{mol}}(X) + \sum_X H_{\text{int}}(X) \tag{2.1}$$

where H_{rad} is the Hamiltonian for the radiation field [explicitly presented in Eq. (2.4) and $H_{\text{mol}}(X)$ is the Hamiltonian for the molecule X, with summations taken over all the molecules of the system. Note that the term *molecule* is used here generically to encompass other electrically neutral species as well, such as atoms. The coupling between the molecular subsystem and the quantized field is represented by a set of terms $H_{\text{int}}(X)$ describing interaction of the field with the individual molecules. For present purposes it is sufficient to express the interaction terms in the electric dipole approximation, though the formalism we employ is perfectly amenable to the incorporation of higher mutipole terms [30]. Thus we write

$$H_{\text{int}}(X) = -\varepsilon_0^{-1} \boldsymbol{\mu}(X) \cdot \mathbf{d}^{\perp}(\mathbf{R}_X) \tag{2.2}$$

where $\boldsymbol{\mu}(X)$ is the electric dipole operator of the molecule X positioned at $\mathbf{R}_X$ and $\mathbf{d}^{\perp}(\mathbf{R}_X)$ is the electric displacement field operator at the molecular site. The latter displacement operator and the radiation Hamiltonian may be cast as [96]:

$$\mathbf{d}^{\perp}(\mathbf{R}) = i \sum_{\mathbf{k},\lambda} \left(\frac{\hbar c k \varepsilon_0}{2V} \right)^{1/2} \mathbf{e}^{(\lambda)}(\mathbf{k}) \{ a^{(\lambda)}(\mathbf{k}) e^{i\mathbf{k}.\mathbf{R}} - a^{(\lambda)^+}(\mathbf{k}) e^{-i\mathbf{k}.\mathbf{R}} \} \tag{2.3}$$

and

$$H_{\text{rad}} = \sum_{\mathbf{k},\lambda} \left[a^{(\lambda)^+}(\mathbf{k}) a^{(\lambda)}(\mathbf{k}) \hbar c k + \frac{1}{2} \right] \tag{2.4}$$

where in each expression a sum is taken over radiation modes characterized by wavevector $\mathbf{k}$ and polarization vector $e^{(\lambda)}(\mathbf{k})$ (with $\lambda = 1, 2$); $a^{(\lambda)+}(\mathbf{k})$ and $a^{(\lambda)}(\mathbf{k})$ are the corresponding operators for creation and annihilation of a photon, and V is an arbitrarily large quantization volume.

B. Resonance Energy Transfer

We shall deal with the resonance ET between a selected pair of species (to be referred to as donor and acceptor) labeled D and A. For this purpose, the full system will be divided into two parts, one subsystem consisting of the transfer species D and A, and the other referred to as the *radiative (polariton) bath*. The latter bath comprises the quantized electromagnetic field and the remaining molecules that constitute the surrounding medium. Note that the molecules of the medium may, but do not necessarily, differ in type from the donor and the acceptor. With regard to the chosen partitioning of the system, the full Hamiltonian (2.1) splits into the zero-order Hamiltonian H^0 and the interaction term V, as

$$H = H^0 + V \tag{2.5}$$

with

$$V = H_{\text{int}}(D) + H_{\text{int}}(A) \tag{2.6}$$

and

$$H^0 = H_{\text{bath}} + H_{\text{mol}}(D) + H_{\text{mol}}(A) \tag{2.7}$$

and where

$$H_{\text{bath}} = H_{\text{rad}} + \sum_{X \neq D,A} [H_{\text{mol}}(X) + H_{\text{int}}(X)] \tag{2.7'}$$

is the "bath" Hamiltonian containing the radiation Hamiltonian H_{rad} and contributions from all molecules other than the donor and the acceptor.

To represent the ET from the donor to the acceptor, the initial and final statevectors are chosen to be the following eigenvectors of the zero-order Hamiltonian H^0:

$$|I\rangle = |D^*\rangle|A\rangle|0\rangle, \qquad |F\rangle = |D\rangle|A^*\rangle|0\rangle \tag{2.8}$$

where the corresponding eigenenergies are

$$E_I = e_{D^*} + e_A + e_{\text{vac}}, \qquad E_F = e_D + e_{A^*} + e_{\text{vac}} \tag{2.9}$$

and $|0\rangle$ represents the ground state of the polariton bath. Note that the subsequent calculation of the transition matrix element (Section II.C) is not affected

if the quantity $|0\rangle$ is replaced by any other radiative statevector characterized by a definite number of medium-dressed photons.* The modifications can emerge only in the fourth order of perturbation [101], which is beyond of the scope of the present analysis. In is intructive that the same radiative part $|0\rangle$ enters the initial and final statevectors [Eq. (2.8)], representing the ET. The change in the radiative state would lead to the higher-order bimolecular processes, such as the single-photon cooperative absorption [66–70] or emission [71].

Here e_{vac} is the zero-point energy of the bath; $|D^*\rangle$ and $|D\rangle$ label the initial and final states of the donor, $|A\rangle$ and $|A^*\rangle$ are the corresponding statevectors of the acceptor (where the asterisk refers to a molecule in an electronically excited state), and e_{D^*} and e_A (e_D and e_{A^*}) are the appropriate energies of the donor and acceptor in their initial (final) states. For generality the statevectors of donor and acceptor are considered to implicitly contain vibrational contributions that are normally separable from the electronic parts on the basis of the Born–Oppenheimer principle, both for the ground and excited electronic molecular states. The vibronic sublevels are explicitly included in the theory in Section IV.A.

It is noteworthy that conventional (semiclassical) theories of radiationless ET [6,8–11] do not invoke any photon states, and the ET appears as a first-order process induced by an instantaneous Coulomb interaction. Such an approach is justified in the near zone, when the distance R of donor–acceptor separation is much less than the reduced wavelength of light $\lambda\!\!\!^{-} = \lambda/2\pi$, where λ is the wavelength of light corresponding to the transfer energy. In the QED formalism employed here, the quantized electromagnetic field is treated on an equal footing to the molecular subsystem, both subsystems comprising a united dynamical system described by the full Hamiltonian H.

C. Transfer Rates

Let us suppose that the process can be described in terms of transfer rates, a condition satisfied by weakly coupled (i.e., most) ET systems. The detailed criteria for this assumption and extensions of the analysis beyond the rate regime are considered in Section VI. The rate of ET, associated with the initial and final states (2.8), can generally be written using the Fermi golden rule (see Section VI for more detail and Refs. 1 and 102 for examples):

$$W_{FI} = \frac{2\pi}{\hbar}|\langle F|T|I\rangle|^2\delta(E_I - E_F) \tag{2.10}$$

* RDDI is not altered in the squeezed radiative vacuum as well [100].

where T is the transition operator:

$$T = T^{(1)} + T^{(2)} + \cdots = V + V\frac{1}{E_I - H^0 + is'}V + \cdots, \qquad s' \to +0 \quad (2.11)$$

where the higher-order terms can for our purposes be neglected. The first-order term $T^{(1)} \equiv V$ does not contribute to the transfer rate in the multipolar formulation of QED employed: such a term describes processes involving the emission or absorption of a medium-dressed photon accompanied by transitions of individual molecules (see Fig. 1). It is the second-order contribution $T^{(2)}$ that is the leading term responsible for the resonance ET in question, a process involving changes in quantum states of both species D and A without alteration of the state of the radiative bath.

Using Eqs. (2.4)–(2.9), the second-order transition matrix element reads

$$\langle F|T^{(2)}|I\rangle = \frac{1}{\hbar}\sum_{\sigma}\sum_{q=1}^{2}\frac{\langle F|V|M_q(\sigma)\rangle\langle M_q(\sigma)|V|I\rangle}{(-1)^{q+1}\omega_{D^*} - \Pi_\sigma + is}, \qquad s \to +0 \quad (2.12)$$

where

$$\hbar\omega_{D^*} \equiv e_{D^*} - e_D = e_{A^*} - e_A > 0 \quad (2.13)$$

is the excitation energy of the donor (as gained by the acceptor) and

$$\hbar\Pi_\sigma = e_\sigma - e_{\text{vac}} \quad (2.14)$$

is the difference in energies between the excited and ground states of the bath. Here also $|M_q(\sigma)\rangle$ denote intermediate states in which both the donor and the

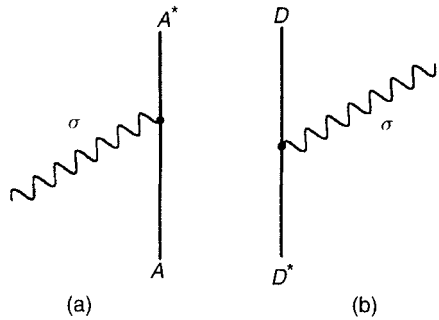

FIGURE 1. Time-ordered diagrams for (*a*) photoabsorption and (*b*) photoemission of a medium-dressed photon labeled by index σ.

acceptor are either in the ground ($q = 1$) or in the excited ($q = 2$) electronic states:

$$|M_1(\sigma)\rangle = |D\rangle|A\rangle|\sigma\rangle \tag{2.15}$$

and

$$|M_1(\sigma)\rangle = |D^*\rangle|A^*\rangle|\sigma\rangle \tag{2.16}$$

where $|\sigma\rangle$ labels the excited states of the radiative bath that are accessible though a single action of the interaction operator V on the ground-state vector $|0\rangle$. Accordingly, the ET is generally regarded as being mediated by such elementary excitations (the bath polaritons) representing photons "dressed" by the material medium.

The two types of intermediate state $|M_q(\sigma)\rangle$ ($q = 1,2$) correspond to the two possible sequences of transitions undergone by the donor and acceptor. In the first case ($q = 1$), the transition $D^* \rightarrow D$ precedes the transition $A \rightarrow A^*$, as depicted in Fig. 2*a*, whereas in the second case ($q = 2$) one has the opposite ordering (Fig. 2*b*). The latter sequence describes an apparently anomalous situation where the upward transition of the acceptor A is accompanied by the creation of a virtual polariton σ, and the subsequent annihilation of the polariton induces the downward transition by the donor $D^* \rightarrow D$. Nevertheless, both types of transition must be included in the theory according to the normal rules of time-dependent perturbation theory. The contribution associated with Fig. 2*b* plays an important role in the near zone, where the uncertainty in energy of a mediating polariton greatly exceeds the excitation energy transferred.

Substituting Eqs. (2.2), (2.8), (2.9) and (2.14)–(2.16) into Eq. (2.12), one arrives at the following expression for the transition matrix element:

$$\langle F|T^{(2)}|I\rangle = \mu_{A_l}^{\text{full}}\theta_{lj}(\omega_{D^*}, \mathbf{R})\mu_{D_j}^{\text{full}} \tag{2.17}$$

where implied summation is assumed over the repeated Cartesian indices l and j, and where

$$\theta_{lj}(\omega, \mathbf{R}) = \frac{1}{\hbar\varepsilon_0^2}\sum_{\sigma}\left[\frac{\langle 0|\mathrm{d}_l^{\perp}(\mathbf{R}_A)|\sigma\rangle\langle\sigma|\mathrm{d}_j^{\perp}(\mathbf{R}_D)|0\rangle}{\omega - \Pi_\sigma + is} - \frac{\langle 0|\mathrm{d}_j^{\perp}(\mathbf{R}_D)|\sigma\rangle\langle\sigma|\mathrm{d}_l^{\perp}(\mathbf{R}_A)|0\rangle}{\omega + \Pi_\sigma - is}\right]$$
$$(\mathbf{R} = \mathbf{R}_A - \mathbf{R}_D) \tag{2.18}$$

is the tensor for the resonance dipole–dipole interaction (RDDI) between a pair of molecules within the medium. The retarded tensor $\theta_{lj}(\omega, \mathbf{R})$ is influenced by the material medium through the yet unspecified intermediate polariton

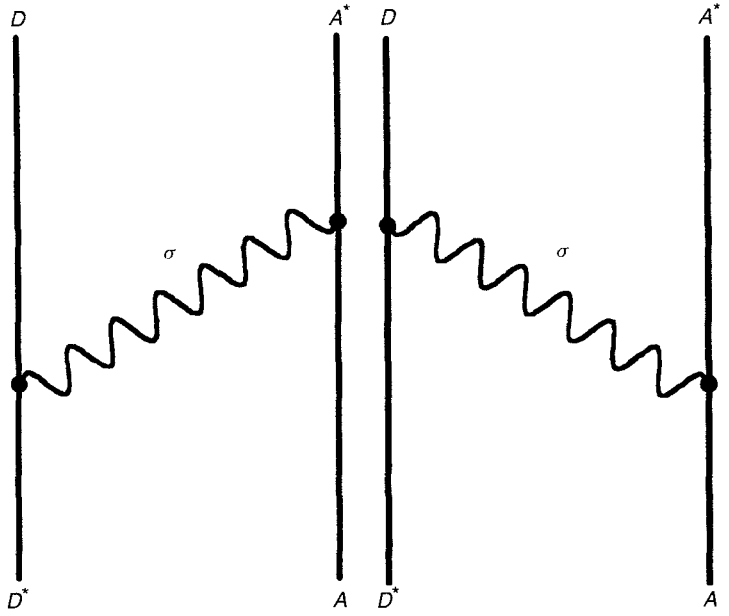

FIGURE 2. The two time-ordered diagrams for resonance ET, time progressing upward. In both cases the transfer of energy from the initially excited donor D^* to the acceptor A is mediated by a photon "dressed" by the medium (virtual polariton), as labeled by index σ.

states σ featured in Eq. (2.18). Here also

$$\boldsymbol{\mu}_D^{\text{full}} = \langle D|\boldsymbol{\mu}(D)|D^*\rangle, \qquad \boldsymbol{\mu}_A^{\text{full}} = \langle A^*|\boldsymbol{\mu}(A)|A\rangle \tag{2.19}$$

are the transition dipole moments of the donor and acceptor, respectively. The superscript "full" indicates that the molecular state vectors entering the transition dipoles (2.19) contain both electronic and vibrational contributions, as made explicit later.

III. ANALYSIS OF THE RDDI TENSOR $\theta_{ij}(w, R)$

A. Vacuum Case

We commence the analysis of the RDDI tensor with the simplest case, where the transfer species are situated in the electromagnetic vacuum. Calculations of a similar kind can be traced back to the papers by Stephen [35], Avery [15], Gomberoff and Power [16], and others [17–21]. In such a vacuum case, the bath Hamiltonian reduces to that of the "free" radiation field, $H_{\text{bath}} = H_{\text{rad}}$, in

which the corresponding eigenstates and eigenenergies take the form

$$|\sigma\rangle = |\mathbf{k}, \lambda\rangle = a^{(\lambda)^+}(\mathbf{k})|0\rangle \tag{3.1}$$

and

$$\Pi_\sigma = \omega_k = ck \tag{3.2}$$

where the state vector $|0\rangle$ now describes the electromagnetic vacuum. Here the intermediate (virtual) photons are considered to be the plane waves characterized by the wavevector $\mathbf{k}$ and polarization λ. One can alternatively represent the intermediate photons in terms of spherical harmonics [38]; however, this does not alter the results.

Calling on Eq. (2.3) for the displacement operator and performing summation over the photon polarizations ($\lambda = 1, 2$), the tensor (2.18) reduces to

$$\theta_{lj}(\omega, \mathbf{R}) \equiv \theta_{lj}^{vac}(\omega, \mathbf{R}) = \sum_{\mathbf{k}} \frac{(\delta_{lj} - \hat{k}_l\hat{k}_j)\omega_k}{2\varepsilon_0 V}\left[\frac{e^{i\mathbf{k}\cdot\mathbf{R}}}{\omega - \omega_k + is} - \frac{e^{-i\mathbf{k}\cdot\mathbf{R}}}{\omega + \omega_k + is}\right] \tag{3.3}$$

Here $\hat{\mathbf{k}} = \mathbf{k}/k$ labels a unit vector along the wavevector $\mathbf{k}$, where the sign of the imaginary infinitesimal is reversed in the second (nonresonant) term of Eq. (3.3). Replacing the summation over $\mathbf{k}$ by an integral and performing the angular integration, Eq. (3.3) takes the form

$$\theta_{lj}^{vac}(\omega, \mathbf{R}) = \frac{1}{16\pi^2\varepsilon_0}\int_0^\infty k^2\,\mathrm{d}k\left[\frac{\omega_k}{\omega - \omega_k + is} - \frac{\omega_k}{\omega + \omega_k + is}\right]\tau_{lj}(k, R) \tag{3.4}$$

with

$$\tau_{lj}(k, R) = \left[(\delta_{ij} - \hat{R}_i\hat{R}_j)\frac{\sin(kR)}{kR} + (\delta_{ij} - 3\hat{R}_i\hat{R}_j)\left(\frac{\cos(kR)}{k^2R^2} - \frac{\sin(kR)}{k^3R^3}\right)\right] \tag{3.5}$$

Since $\omega_{-k} = -\omega_k$ and $\tau_{lj}(-k, R) = \tau_{lj}(k, R)$, the integration contour can be expanded to negative values of k in Eq. (3.4), subsequently closing it up by a large semicircle on the upper or lower complex half-plane [depending on the sign of the exponents comprising the geometric functions in Eq. (3.5)]. Calculating the residues at $k = \pm(\omega + is)/c$, one arrives at the final result for the retarded RDDI tensor in vacuum for $R \neq 0$:

$$\theta_{ij}^{vac}(\omega, \mathbf{R}) = \frac{\omega^3 e^{iKR}}{4\pi\varepsilon_0 c^3}\left[(\delta_{ij} - 3\hat{R}_i\hat{R}_j)\left(\frac{c^3}{\omega^3R^3} - \frac{ic^2}{\omega^2R^2}\right) - (\delta_{ij} - \hat{R}_i\hat{R}_j)\frac{c}{\omega R}\right] \tag{3.6}$$

where use has been made of the dispersion relationship (3.2).

The above tensor contains an R^{-3} term characteristic of the near-zone ($\omega R/c \ll 1$), a radiative R^{-1} term operating in the far zone ($\omega R/c \gg 1$), as well as an R^{-2} contribution manifesting at critical retardation distances: $\omega R/c \cong 1$. In calculating the RDDI tensor, an important role is played by the imaginary infinitesimal "*is*" featured in Eq. (2.12) for the transition matrix element, and in the subsequent equations. It is noteworthy that such an infinitesimal emerges intrinsically from the time-dependent analysis of the problem (to be considered explicitly in Section VI). It is the presence of the imaginary infinitesimal that ensures the correct bypassing of a pole in Eqs. (3.4). Thus one automatically avoids analytic problems [19] associated with the choice of the integration contour.

Note, too, that in some studies, such as Ref. 96, the RDDI tensor (and hence the transition matrix element) has been calculated by taking the principal part of the integral: this corresponds to the real part of the RDDI tensor given by Eq. (3.6). In the near zone, the real part of the transition matrix element describes the shift in excitation energy for a pair of species coupled via the resonant dipole–dipole interaction, although such an interpretation can be inappropriate in the far zone [35].

B. Photonic Bandgap Structures

Analysis of the RDDI tensor for photonic bandgap crystals is generally a tough problem. In such structures the photons are characterized by a much more complex dispersion relationship ω_k compared to that in vacuum, and the mode functions are now spatially modulated [103]. The spatial modulation renders the transfer energy sensitive to the specific sites of the transfer species within an elementary cell of the photonic bandgap crystal (the superlattice) [75].* In order to establish some characteristic features of the RDDI coupling in photonic bandgap crystals, we neglect the spatial modulation [71,76], assuming the photon modes to represent transverse plane waves. Under this condition, one can repeat the preceding analysis of the vacuum case up to Eqs. (3.4) and (3.5), in which ω_k is now understood as a dispersion relationship for a photon in a bandgap structure.

Various forms have been used to represent the dispersion of ω_k. Kweon and Lawandy [76] adopted the vacuum dispersion $\omega_k = ck$ everywhere except a range of frequency magnitudes $\omega_0 \pm \delta\omega$ where no modes exist, and the center of the bandgap ω_0 was chosen to coincide with the transfer frequency ω_{D^*}. On the other hand, John and Wang [71] employed another form of photon

* The site-sensitivity features also for the RDDI in Mie particles [82–86], in waveguides [76], and for a system restricted by the two mirrors [80].

dispersion:

$$\omega_k = \frac{c}{4na}\arccos\left[\frac{4n\cos(kL) + (1-n)^2}{(1+n)^2}\right] \tag{3.7}$$

which follows from the isotropic model for electromagnetic waves in a three-dimensional periodic dielectric. Here n is the refractive index of the scatterer, a is its radius, and $2a + b = L$ is the constant of the superlattice; furthermore, Eq. (3.7) corresponds to the special case where $2na = b$. The function ω_k has branchcut singularities at $k = m\pi/L$, the bandgaps appearing for odd values of m, as illustrated in Fig. 3.

Calculations [71,76] have shown that the suppression of the RDDI can be appreciable only in the far zone: $\omega R/c \gg 1$, whereas the transition matrix element appears to be close to its vacuum values in the near zone. In fact, the precision with which the law of energy conservation has to apply to the virtual photons is determined by the time–energy uncertainty principle: $\delta E \delta t \geq \hbar$, where δt is the time necessary for a photon to cover the distance between the donor and the acceptor. In the near zone ($\omega R/c \ll 1$), the uncertainty in energies of virtual photons is large: $\delta E \gg \hbar\omega$, so that the presence of the bandgap makes little difference to the RDDI tensor.

In the far zone ($\omega R/c \gg 1$) one has the opposite effect: $\delta E \ll \lambda cK$, so that the virtual photon acquires a somewhat real character. As a result, the absence

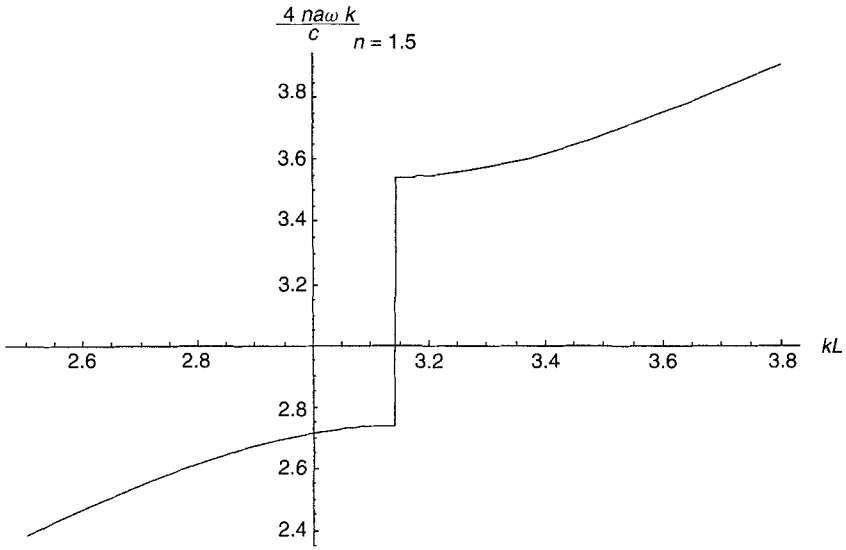

FIGURE 3. Dispersion relationship for a photon in an isotropic bandgap structure, calculated using Eq. (3.7).

of resonant photons can considerably diminish the transition matrix element for the excitation ET in the far zone.

To illustrate this fact, we shall present the analytic expressions for the RDDI tensor [and hence the transition matrix element given by Eq. (2.17)] by using the *effective-mass* approximation for the photon dispersion [71], this is appropriate for transition frequencies very close to the photonic bandedge and for far-zone distances $KR \gg 1$. Expanding Eq. (3.7) around the upper bandedge ω_c one has [71]:

$$\omega_k \approx \omega_c + A(k - k_c)^2 \tag{3.8}$$

where $k_c = \pi/L$,

$$\omega_c = \frac{c}{4na}\left[2\pi - \cos^{-1}\left(\frac{1 - 6n + n^2}{1 + 2n + n^2}\right)\right] \tag{3.9}$$

and

$$A = \frac{-cL^2}{2a(1+n)^2}\frac{1}{\sin(4na\omega_c/c)} \tag{3.10}$$

Substituting the dispersion (3.8) into Eq. (3.4), the RDDI tensor takes the following form for $KR \gg 1$

$$\theta_{lj}(\omega, \mathbf{R}) = -(\delta_{lj} - \hat{R}_l\hat{R}_j)\frac{i\omega_0 k_c \sin(k_c R)}{16\pi\varepsilon_0\sqrt{A(\omega_c - \omega)}}\frac{e^{-R/\xi}}{R} \tag{3.11}$$

where

$$\xi = \sqrt{A/(\omega_c - \omega)} \tag{3.12}$$

can be interpreted [71,104] as the length of photon localization around embedded atoms or molecules. Near the bandedge, the localization length considerably exceeds the reduced wavelength: $\xi \gg \lambda\!\!\!^{-} = c/\omega$. Consequently, efficient ET can take place over far-zone distances up to the localization length, the process being ensured by the overlap of spatially extended clouds of virtual photons surrounding both donor and acceptor.

It is noteworthy that the straightforward application of the effective-mass approximation to the near-zone distances leads to a drastic modification of the RDDI [75]. Such an approach has been criticized by John and Wang [71], who pointed out that the effective-mass approximation is not applicable for the distance scales $KR \ll 1$. In fact, here the uncertainty in energies of virtual photons is large, so the relevant intermediate photons are no longer restricted to the bandedge. Note also that Refs. 71 and 76 (as well as other studies [77–78,105] on the resonance ET in the photonic bandgap crystals) are based

on the isotropic model for the photon dispersion. Such a model overestimates the number of photon states near the bandedge.

Finally, we briefly mention recent analysis of the temporal behavior of excitation exchange between a pair of atoms in high-Q cavities [77,87] and in photonic bandgap crystals [77]. Such a process might be completely different from the one occurring in vacuum or in dielectric media (away from the exciton resonances). In fact, even in the single-center case, the rapidly varying density of radiative modes leads to nonexponential spontaneous atomic decay [92,93,106–108] in cavities or photonic crystals. For instance, for atomic frequencies close to the bandedge, the splitting of the atomic level (vacuum Rabi splitting) [71,104] leads to oscillatory spontaneous decay [92]. In the case of a two-center system, the kinetics can be even more complicated [77,87], the vacuum Rabi splitting now competing with the RDDI.

In what follows we shall concentrate on the quantum electrodynamics of energy transfer in dielectric media.

C. RDDI in Dielectric Media

We consider next, without making any phenomenological assumptions, the form of the RDDI in a discrete molecular medium. For this purpose, let us return to the general relationship (2.18) for the tensor $\theta_{lj}(\omega, \mathbf{R})$ in which the influences of the material medium arise through the intermediate polariton states labeled by the index σ. The analysis of the intermediate states can be bypassed in calculating the RDDI tensor by invoking the Green function formalism [27]. As an alternative, one can make use of the explicit mode expansion of the operators for the local displacement field entering Eq. (2.18). Such a mode expansion has been recently derived by Juzeliūnas, giving [109–111]

$$\mathbf{d}^{\perp}(\mathbf{R}_X) = i \sum_{\mathbf{k}} \sum_{m=1}^{M+1} \sum_{\lambda=1}^{2} \left(\frac{\varepsilon_0 \hbar \omega_k^{(m)} v_g^{(m)}}{2cV_0 n(\omega_k^{(m)})} \right)^{1/2} \left[\frac{[n(\omega_k^{(m)})]^2 + 2}{3} \right] \times \mathbf{e}^{(\lambda)}(\mathbf{k}) (e^{i\mathbf{k}\cdot\mathbf{R}_X} P_{\mathbf{k},m,\lambda} - e^{-i\mathbf{k}\cdot\mathbf{R}_X} P^{+}_{\mathbf{k},m,\lambda}) \tag{3.13}$$

with $(\mathbf{k}, m, \lambda) \equiv \sigma$ labeling the normal (polariton) modes. Here $P^{+}_{\mathbf{k},m,\lambda}(P_{\mathbf{k},m,\lambda})$ is the Bose operator for creation (annihilation) of a polariton characterized by a wavevector $\mathbf{k}$, a polarization index λ, with an extra index m specifying a dispersion branch, and where

$$\Pi_\sigma \equiv \omega_k^{(m)} = \frac{ck}{n(\omega_k^{(m)})} \tag{3.14}$$

is the polariton frequency in the mth dispersion branch. Here, too, $v_g^{(m)} = \mathrm{d}\omega_k^{(m)}/\mathrm{d}k$ is the branch-dependent group velocity and $n(\omega)$ is the refractive index:

$$[n(\omega)]^2 = 1 + \frac{\alpha(\omega)\rho/\varepsilon_0}{1 - \alpha(\omega)\rho/3\varepsilon_0} \tag{3.15}$$

where ρ is the molecular density and $\alpha(\omega)$ is the molecular polarizability, given by

$$\alpha(\omega) = \frac{1}{\hbar}\sum_{\gamma=1}^{M}\left(\frac{\mu_\gamma^2}{\Omega_\gamma - \omega} + \frac{\mu_\gamma^2}{\Omega_\gamma + \omega}\right) \tag{3.16}$$

The local operator (3.13) has been obtained through the diagonalization of a microscopic Hamiltonian for a discrete molecular medium coupled to a quantized radiation field. The molecules of the medium have been assumed to be all of the same type, regularly placed to form a simple cubic lattice, and characterized by the same isotropic polarizabilities. Such a model is believed to describe fairly well the optical properties of some other isotropic and homogeneous media that are not necessarily ordered, such as a common situation where the nonisotropic species are randomly oriented in their sites.

Equations (3.14)–(3.16) yield $M + 1$ dispersion branches, where M is the number of excitation frequencies Ω_γ accommodated by each molecule forming the medium, and μ_γ is the corresponding transition dipole moment. For instance, the single-frequency (Hopfield) model provides two polariton branches. Examples of dispersion curves with various values of M are presented in Fig. 4. As the number of molecular frequencies increases, the dispersion branches may start to form dense sets, as illustrated in Fig. 4*c*. Hence, the formalism may also adequately accommodate the formation of quasicontinua of vibrational, rotational, and other sublevels in the molecular spectra. This makes the approach applicable to both lossless and absorbing media. It is noteworthy that a similar multifrequency model of the medium has been considered very recently by Drummond and Hillery [113]. Yet, their theory has been restricted to the mode expansion of the macroscopic field operators. On the other hand, Juzeliūnas treated the operators for local [109–111], microscopic [111], and macroscopic [110] fields. It is the operator for the local displacement field that describes various molecule–radiation processes [109] in condensed media including, inter alia, the resonance ET.

The expansion (3.13) extends to the modes characterized by relatively large wavelength:

$$k \ll \frac{2\pi}{a} \tag{3.17}$$

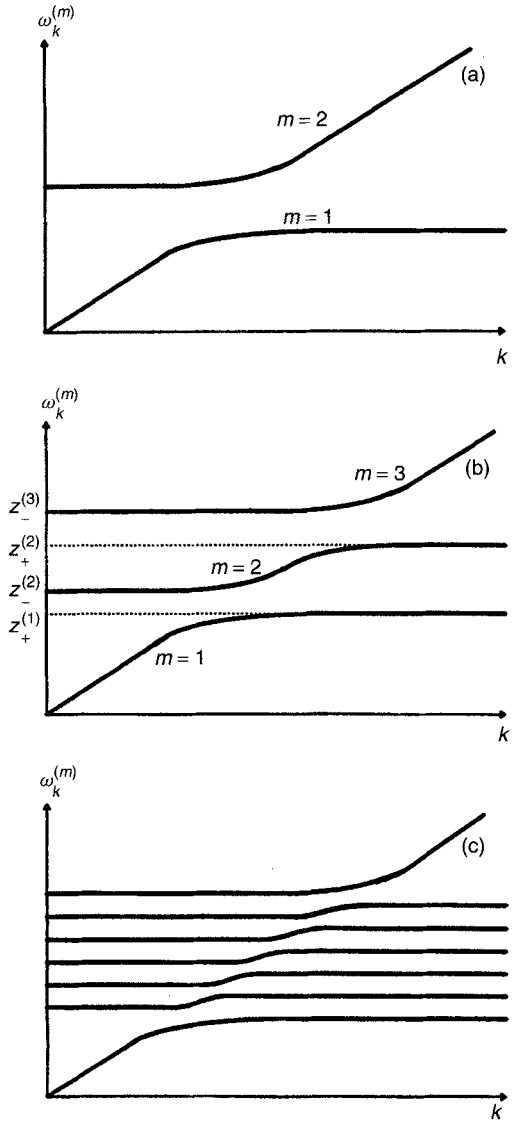

FIGURE 4. Schematic plot of the dispersion curves $\omega_k^{(m)}(m = 1, \ldots, M + 1)$ for (a) $M = 1$ (Hopfield model) and (b) $M = 2$; the third diagram (c) illustrates a situation in which a dense set of dispersion curves is featured. Note that all the diagrams represent the long-wavelength region of the spectrum ($k \ll 2\pi/a$) of interest. For greater values of k, the effects of spatial dispersion are to be considered. The quantities $z = z_+^{(m)}$ and $z = z_-^{(m)}$ label the upper and lower boundaries of polariton bands, for which $n(z_+^{(m)}) = \infty$ and $n(z_-^{(m)}) = 0$, respectively. Diagrams (a)–(c) have been reproduced from a paper by G. Juzeliūnas (Ref. 110) with the kind permission of the American Physical Society.

with the lattice constant $a = \rho^{-1/3}$ representing a characteristic distance between the molecules constituting the medium. Under this condition, the expanded displacement operator (3.13) is described exclusively in terms of the refractive index. The excluded short-wavelength modes play little role in the formation of the RDDI between donor and acceptor, as long as their separation distance R is large compared to a.

It is noteworthy that the mode expansion (3.13) holds for the local displacement field operator calculated both at a lattice site [109,110] and also at an intersitial location. This has been demonstrated in Appendix A using the mode expansions of microscopic field-operators derived in Ref. [111].* It is instructive that the (virtual cavity) local field factors explicitly feature in the microscopically derived mode expansion (3.11) of the local operator, leading to the appropriate local field corrections in the subsequent equations (3.18), (4.9), (4.10), (5.1), and (5.14).

Substituting Eq. (3.13) for $\mathbf{d}^{\perp}(\mathbf{R}_X)$ (with $X = D, A$) into Eq. (2.18), and performing the appropriate summation over the intermediate states, the RDDI tensor takes the form (see Appendix B):

$$\theta_{lj}(\omega, \mathbf{R}) = \frac{1}{n^2}\left(\frac{n^2+2}{3}\right)^2 \theta_{lj}^{vac}(n\omega, \mathbf{R}) \tag{3.18}$$

where $\theta_{lj}^{\mathrm{vac}}$ is the vacuum RDDI tensor given by Eq. (3.6). The relationship (3.18) is equivalent to the result by Juzeliūnas and Andrews [27] obtained using the Green function technique. The tensor (3.18) accommodates a screening contribution n^{-2} and a local field (Lorenz) factor $(n^2+2)/3$. In addition, the argument of the vacuum tensor $\theta_{lj}^{vac}(n\omega, \mathbf{R})$ is now scaled by the complex refractive at the frequency ω:

$$n \equiv n(\omega + is) = n' + in'' \tag{3.19}$$

Note that in the present formalism, the initial refractive index $n(\omega_k^{(m)})$ entering the mode expansion (3.13) is a real branch-dependent quantity. In fact the poles of $n(\omega)$, given by (3.15), emerge at frequencies other than the eigenfrequencies $\omega_k^{(m)}$, so $n(\omega_k^{(m)})$ is a well-defined quantity without adding any imaginary part to the argument $\omega_k^{(m)}$. On the other hand, the refractive index $n \equiv n(\omega + is)$, featured in the RDDI tensor, would be ill-defined within the absorbing regions if a strict mathematical limit $s \to +0$ were taken. That

* A somewhat similar conclusion has been reached by De Vries and Lagendijk in their theory of resonant scattering of classical light by impurity atoms inside dielectric cubic lattices [112]. It has been demonstrated [112] that the local field factors associated with a virtual cavity apply for molecules in pure systems and for intersital impurities.

is why the quantity s is to be regarded as a finite (although small) parameter reflecting the natural widths of each molecular line; the replacement of an infinitesimal s by its finite counterpart can be justified on rigorous dynamical grounds, as discussed in Section VI. In the absorbing areas of the spectrum, the width s is considered to be larger than the characteristic distance between the densely spaced (quasicontinuum) molecular sublevels of vibrational or other origin. This makes the refractive index a smooth quantity containing a finite imaginary part in the absorbing areas.

IV. ENERGY TRANSFER IN A DIELECTRIC MEDIUM

A. Inclusion of the Vibrational Structure for the Transfer Species

Up to now the vibrational structure has been kept implicit for the molecular state vectors of donor and acceptor. To explicitly display the vibrational sublevels, we make use of the Born–Oppenheimer approximation [114], according to which the molecular state vectors are separated into electronic and vibrational parts, as

$$|D^*\rangle = |D^*_{\mathrm{el}}\rangle|\varphi^{(n)}_{D^*}\rangle, \qquad |D\rangle = |D_{\mathrm{el}}\rangle|\varphi^{(r)}_{D}\rangle \tag{4.1}$$

$$|D\rangle = |A_{\mathrm{el}}\rangle|\varphi^{(m)}_{A}\rangle, \qquad |A^*\rangle = |A^*_{\mathrm{el}}\rangle|\varphi^{(p)}_{A^*}\rangle \tag{4.2}$$

where the subscript "el" refers to the electronic part of the state vectors and the indices n, r, m, and p specify the vibrational, rotational, and other sublevels of the transfer species D and A. The transition dipole moments (2.19) then split into electronic and vibrational contributions, as:

$$\boldsymbol{\mu}_D^{full} = \langle D_{\mathrm{el}}|\boldsymbol{\mu}(D)|D^*_{\mathrm{el}}\rangle\langle\varphi^{(r)}_{D}|\varphi^{(n)}_{D^*}\rangle \equiv \boldsymbol{\mu}_D\langle\varphi^{(r)}_{D}|\varphi^{(n)}_{D^*}\rangle \tag{4.3}$$

$$\boldsymbol{\mu}_A^{full} = \langle A^*_{\mathrm{el}}|\boldsymbol{\mu}(A)|A_{\mathrm{el}}\rangle\langle\varphi^{(p)}_{A^*}|\varphi^{(m)}_{A}\rangle \equiv \boldsymbol{\mu}_A\langle\varphi^{(p)}_{A^*}|\varphi^{(m)}_{A}\rangle \tag{4.4}$$

where, according to the Condon principle, the dipole operators of the donor and acceptor, $\boldsymbol{\mu}(D)$ and $\boldsymbol{\mu}(A)$, respectively, are assumed not to depend on the vibrational degrees of freedom, where $\boldsymbol{\mu}_D$ and $\boldsymbol{\mu}_A$ are the appropriate electronic parts of the transition dipoles.

Substituting the transition dipoles (4.3) and (4.4) into Eq. (2.17), the full rate of donor–acceptor transfer reads — after performing the necessary averaging over the initial molecular states and summing over the final molecular states in Eq. (2.10)

$$W_{DA} = \frac{2\pi}{\hbar}\sum_{n,m,r,p}\rho^{(n)}_{D^*}\rho^{(m)}_{A}|\langle\varphi^{(r)}_{D}|\varphi^{(n)}_{D^*}\rangle\langle\varphi^{(p)}_{A^*}|\varphi^{(m)}_{A}\rangle|^2|\mu_{A_l}\mu_{D_j}|^2$$
$$\times\,|\theta_{lj}(\omega_{D^*_{nr}}, \mathbf{R})|^2\delta(\hbar\omega_{D^*_{nr}} - \hbar\omega_{A^*_{pm}}) \tag{4.5}$$

Here $\rho_{D^*}^{(n)}$ and $\rho_A^{(m)}$ are the population distribution functions of the initial vibrational states of the donor and the acceptor, respectively; the vibrational indices are also included in the excitation energies of donor and acceptor ($\hbar\omega_{D^*_{nr}} \equiv \hbar\omega_{D^*} = e_{D^*_n} - e_{D_r}$ and $\hbar\omega_{A^*_{pm}} \equiv \hbar\omega_{A^*} = e_{A^*_p} - e_{A_m}$) that feature in the energy-conserving delta function.

Using Eqs. (3.18) and (3.6) for the RDDI tensor in the dielectric medium, the pair rate (4.5) can be expressed in terms of the overlap integral between the donor and acceptor spectra:

$$W_{DA} = \frac{9}{8\pi c^2 \tau_D} \int_0^\infty F_D(\omega)\sigma_A(\omega)\omega^2 g(\omega, \mathbf{R}) e^{-2n''\omega R/c} \mathrm{d}\omega \tag{4.6}$$

with

$$\begin{aligned} g(\omega, \mathbf{R}) &= |n|^2 \left| \eta_3 \left[\left(\frac{c}{n\omega R} \right)^3 - i \left(\frac{c}{n\omega R} \right)^2 \right] - \eta_1 \frac{c}{n\omega R} \right|^2 \\ &= \frac{1}{|n|^4} \left\{ \eta_3^2 \frac{c^6}{\omega^6 R^6} + 2\eta_3^2 n'' \frac{c^5}{\omega^5 R^5} + \left[\eta_3^2 |n|^2 - 2\eta_1\eta_3 (n'^2 - n''^2) \right] \right. \\ &\quad \left. \times \frac{c^4}{\omega^4 R^4} + 2\eta_1\eta_3 n'' |n|^2 \frac{c^3}{\omega^3 R^3} + \eta_1^2 |n|^4 \frac{c^2}{\omega^2 R^2} \right\} \end{aligned} \tag{4.7}$$

and where

$$\eta_q = (\hat{\boldsymbol{\mu}}_A . \hat{\boldsymbol{\mu}}_D) - q(\hat{\mathbf{R}} . \hat{\boldsymbol{\mu}}_A)(\hat{\mathbf{R}} . \hat{\boldsymbol{\mu}}_D), \qquad q = 1, 3 \tag{4.8}$$

are the orientational factors (the carets referring to unit vectors), $n \equiv n(\omega + is) = n' + in''$ is the complex refractive index* at frequency ω, and

$$\sigma_A(\omega) = \frac{\pi\omega\mu_A^2}{3\varepsilon_0 c} \frac{1}{n'} \left| \frac{n^2 + 2}{3} \right|^2 \sum_{m,p} \rho_A^{(m)} |\langle \varphi_{A^*}^{(p)} | \varphi_A^{(m)} \rangle|^2 \delta(\hbar\omega_{A^*_{mp}} - \hbar\omega) \tag{4.9}$$

and

$$F_D(\omega) = \frac{\omega^3 \tau_D \mu_D^2}{3\varepsilon_0 \pi c^3} n' \left| \frac{n^2 + 2}{3} \right|^2 \sum_{n,r} \rho_{D^*}^{(n)} |\langle \varphi_D^{(r)} | \varphi_{D^*}^{(n)} \rangle|^2 \delta(\hbar\omega_{D^*_{nr}} - \hbar\omega) \tag{4.10}$$

can be identified (see Section V.B), respectively, as the absorption cross section of the acceptor and the emission spectrum of donor. The latter $F_D(\omega)$

* See the discussion following Eq. (3.19) regarding the introduction of the complex refractive index in the present formalism.

is normalized to unity in the Following sense:

$$\int F_D(\omega)\mathrm{d}\omega = 1 \tag{4.11}$$

It is noteworthy that both $\sigma_A(\omega)$ and $F_D(\omega)$ contain refractive corrections due to the medium, including the local field factors. In this way, dielectric influences of the material medium are introduced into the pair rate (4.6) through the refractive modifications of the spectral functions $F_D(\omega)$ and $\sigma_A(\omega)$, as well as through the factors $g(\omega, \mathbf{R})$ and $e^{-2n''\omega R/c}$. The latter exponential factor represents the Beer law losses in the absorbing medium. This factor will be demonstrated to play a vital role at large separations between the transfer species, providing a physically sensible total rate of ET to all the surrounding acceptors (see Section V.B).

The pair rate (4.6) applies to arbitrary transfer distances, covering both near and far zone, as well as intermediate distances. It can be presented meaningfully as the following sum of three terms:

$$W_{DA} = W_{DA}^{\text{Först}} + W_{DA}^{I} + W_{DA}^{\text{farzone}} \tag{4.12}$$

The first term namely

$$W_{DA}^{\text{Först}} = \frac{9c^4\eta_3^2}{8\pi\tau_D R^6}\int_0^\infty F_D(\omega)\sigma_A(\omega)|n|^{-4}\omega^{-4}\mathrm{d}\omega \tag{4.13}$$

represents the familiar Förster rate of ET characterized by an R^{-6} distance dependence and featuring the orientational factor η_3^2; the latter factor is commonly labaled by κ^2 in the theory of radiationless ET (see, e.g., Ref. 115). The rate $W_{DA}^{\text{Först}}$ is the dominant contribution in the near zone ($|n|\overline{\omega}R/c \ll 1$). Here the exponential factor $e^{-2n''\omega R/c}$ is close to unity and has therefore been disregarded in Eq. (4.13), where $\overline{\omega}$ is an averaged transfer frequency. Consequently, the spectral integral (4.13) is weighted by the factor $|n|^{-4}$ in the near zone, in agreement with the standard theory of radiationless ET [6,11].

The third term in (4.12), namely

$$W_{DA}^{\text{farzone}} = \frac{9\eta_1^2}{8\pi\tau_D R^2}\int_0^\infty F_D(\omega)\sigma_A(\omega)e^{-2n''\omega R/c}\mathrm{d}\omega \tag{4.14}$$

dominating in the far zone ($|n|\overline{\omega}R/c \gg 1$), is characterized by the an R^{-2} behavior corrected by the exponential decay factor. The rate (4.14) has been represented through the overlap integral between the donor emission and acceptor absorption spectra, weighted by the exponential Beer law factor. The result (4.14) can be identified as the rate of radiative (far-zone) ET involving spontaneous emission by a donor, propagation of the emitted photon through

the absorbing medium, followed by its absorption at the acceptor. The factors $F_D(\omega)$, $e^{-2n''\omega R/c}$ and $\sigma_A(\omega)$ characterize the corresponding processes. It is noteworthy that the local field factors are contained in the spectral functions $F_D(\omega)$ and $\sigma_A(\omega)$. Note also that the near and far zone rates differ not only in the distance dependence but also in their orientational factors. This leads to a completely different transfer-induced fluorescence depolarization in these two cases, an issue to be discussed in detail in the following section.

Finally, the middle term of the pair rate (4.12), W^I_{DA}, due to the remaining terms in the function (4.7), becomes important at intermediate distances where $|n|\overline{\omega}R/c \cong 1$. In general this intermediate contribution contains not only the usual R^{-4} term [15–23] but also additional terms in odd powers of R (i.e., R^{-3} and R^{-5}). However, in the case of weakly absorbing medium ($n'' \ll n'$), one can disregard the latter odd rank terms to arrive at the following approximate expression:

$$W^I_{DA} = \frac{9c^2(\eta_3^2 - 2\eta_1\eta_3)}{8\pi\tau_D R^4} \int_0^\infty F_D(\omega)\sigma_A(\omega)|n|^{-2}\omega^{-2}e^{-2n''\omega R/c}\mathrm{d}\omega \qquad (4.15)$$

For such a weakly absorbing medium, the function $g(\omega, \mathbf{R})$ entering the pair rate (4.6) can be written approximately as

$$g(\omega, \mathbf{R}) = |n|^2 \left[\eta_3^2 \left(\frac{c}{|n|\omega R}\right)^6 + (\eta_3^2 - 2\eta_1\eta_3)\left(\frac{c}{|n|\omega R}\right)^4 + \eta_1^2\left(\frac{c}{|n|\omega R}\right)^2\right] \qquad (4.16)$$

Note that in most situations the media are indeed weakly absorbing. The condition $n'' \ll n'$ can fail only near sharp resonances of the medium. Yet, in such a case the whole idea of description of the ET in terms of transfer rates is to be questioned.

We conclude this section with a brief remark concerning nonrigid systems having fast rotational motion of the donor and the acceptor. In such a situation the factor $g(\omega, \mathbf{R})$ given above should be replaced by its orientational average:

$$g_{av}(\omega, \mathbf{R}) = \frac{2}{9}|n|^2 \left[3\left(\frac{c}{|n|\omega R}\right)^6 + \left(\frac{c}{|n|\omega R}\right)^4 + \left(\frac{c}{|n|\omega R}\right)^2\right] \qquad (4.17)$$

B. Range Dependence of the Fluorescence Depolarization Due to ET

In this section we analyze the range dependence of the fluorescence depolarization, applying the unified approach to the radiationless and radiative ET.* For

* This issue has been first addressed in Ref. 23 neglecting the effects of the surrounding medium. Here we include the medium effects as well.

the near-zone (nonradiative) ET, the transfer rate depends only weakly on the average mutual orientation of the donors and acceptors [see Eq. (4.19) for the average of the appropriate orientational factor]. This is the reason for the well-known and considerable ($\frac{1}{25}$) reduction of fluorescence anisotropy following a single act of ET in an isotropic or randomly oriented system [6,11]. By contrast in the radiative mechanism, the ET between molecules with parallel transition dipoles is greatly preferred—as one can see from Eq. (4.18), in which the angle-dependent term is weighted by a factor of 7. This leads to a substantially smaller loss of polarization for an ensemble of randomly oriented transfer species; specifically, the residual anisotropy following a single act of photon reabsorption is 7 times greater than in the case of the short-range (nonradiative) ET.

Here we present a general result for the residual fluorescence anisotropy that connects and accommodates the two limiting cases, also providing the behavior at the intermediate distances where neither radiative nor radiationless mechanism dominates. Note that the rotational depolarization is assumed to be negligible. In order to obtain a formula exhibiting the effects of the relative donor-acceptor orientation in an ensemble, it is necessary to average the pair rate (4.6) over the orientation of the radius vector $\mathbf{R}$ keeping a fixed mutual orientation between donor and acceptor. We then arrive at the following rotational averages of the orientational factors featured in the function $g(\omega, \mathbf{R})$ entering the rate (4.6):

$$\langle \eta_1^2 \rangle = \tfrac{1}{15}(7\cos^2\theta + 1) \tag{4.18}$$

$$\langle \eta_3^2 \rangle = \tfrac{1}{5}(\cos^2\theta + 3) \tag{4.19}$$

and

$$\langle \eta_1 \eta_3 \rangle = \tfrac{1}{3}\langle \eta_3^2 \rangle \tag{4.20}$$

where $\cos\theta = \hat{\boldsymbol{\mu}}_A \cdot \hat{\boldsymbol{\mu}}_D$.

We shall concentrate on the situation where a medium is sufficiently weakly absorbing that one can make use of Eq. (4.16) for the function $g(\omega, \mathbf{R})$. Substituting the averages (4.18)–(4.20) into Eqs. (4.6) and (4.16), we then obtain the following orientationally averaged rate, for the case of a fixed angle θ between the transition dipoles of donor and acceptor:

$$\langle W(R) \rangle \propto (3y_6 + y_4 + 7y_2)\cos^2\theta + (9y_6 + 3y_4 + y_2) \tag{4.21}$$

where the range characteristics y_n are spectral overlap moments of the form

$$y_n = \frac{c^{n-2}}{R^n} \int_0^\infty F_D(\omega)\sigma_A(\omega)|n\omega|^{(2-n)} e^{-2n''\omega R/c} \mathrm{d}\omega, \qquad n = 2, 4, 6 \tag{4.22}$$

Therefore, the properly normalized function for the orientational distribution of excited acceptors is given by

$$f(\theta, R) = \frac{3}{10} \frac{(3 + \overline{k^2}R^2 + 7\overline{k^4}R^4)\cos^2\theta + (9 + 3\overline{k^2}R^2 + \overline{k^4}R^4)}{3 + \overline{k^2}R^2 + \overline{k^4}R^4} \tag{4.23}$$

where the bar over k^2 and k^4 signifies the spectral averages:

$$\overline{k^n} = \frac{\int_0^\infty |n\omega/c|^n F_D(\omega)\sigma_A(\omega)|n\omega|^{-4} e^{-2n''\omega R/c} d\omega}{\int_0^\infty F_D(\omega)\sigma_A(\omega)|n\omega|^{-4} e^{-2n''\omega R/c} d\omega} \tag{4.24}$$

Of special interest is the fluorescence anisotropy commonly defined by

$$r = \frac{I_\parallel - I_\perp}{I_\parallel + 2I_\parallel} \tag{4.25}$$

where $I_\parallel$ and $I_\perp$ are components of the fluorescence intensity polarized, respectively, parallel and perpendicular to the polarization of the excitation light. In the case where fluorescence occurs directly from the molecule that absorbs the incident light (the donor), the anisotropy is designated r_0; where fluorescence occurs following a single-step transfer of energy to another molecule (the acceptor), the anisotropy is designated r_1. The value of r_0 reaches its theoretical maximum of 0.4 if intramolecular relaxation of the donor produces no change of electronic state [6,11].

Here it is the result for r_1 that is of principal interest; the fluorescence anisotropy following a chain of ET events can be directly calculated from this result. In terms of r_0, the acceptor anisotropy r_1 can be expressed as (see, e.g., Ref. 116)

$$r_1 = \langle\langle P_2(\cos\theta)\rangle\rangle r_0 \tag{4.26}$$

where $P_2(\cos\theta) = \frac{1}{2}(3\cos^2\theta - 1)$ is the second-order Legendre polynomial, and the double angular brackets denote the orientational average over the mutual orientations of donor and acceptor:

$$\langle\langle P_2(\cos\theta)\rangle\rangle = \frac{1}{2}\int_0^\pi P_2(\cos\theta) f(\theta) \sin\theta d\theta \tag{4.27}$$

Substituting the distribution function (4.23) into Eq. (4.27), we obtain the following most general result for the fluorescence anisotropy:

$$r_1(R) = \frac{r_0}{25} \frac{7\overline{k^4}R^4 + \overline{k^2}R^2 + 3}{\overline{k^4}R^4 + \overline{k^2}R^2 + 3} \tag{4.28}$$

This equation is valid for arbitrary separations R. As shown in Eqs. (4.34) and (4.35), the familiar near- and far-zone results are the asymptotes of this formula.

In the general case, the residual anisotropy depends not only on the transfer distance but also on the shapes of the spectral lines through the averages $\overline{k^2}$ and $\overline{k^4}$ featured in Eq. (4.28). However, as the widths of the absorption and emission lines are considerably less than the photon frequency, Eq. (4.28) can be rewritten without a significant loss of generality as

$$r_1(R) = \frac{r_0}{25} \frac{7\bar{k}^4 R^4 + \bar{k}^2 R^2 + 3}{\bar{k}^4 R^4 + \bar{k}^2 R^2 + 3} \tag{4.29}$$

where the average wavenumber $\bar{k}$ is related approximately to the averaged transfer frequency $\overline{\omega}$ as

$$\bar{k} = \frac{|n|\overline{\omega}}{c} \tag{4.30}$$

In the case where the absorption and emission lines are of Gaussian shape

$$F_D(\omega) \propto \omega^3 \exp \frac{(\omega - \overline{\omega}_{D^*})^2}{2\sigma^2}, \qquad \sigma_A(\omega) \propto \omega \exp \frac{(\omega - \overline{\omega}_{A^*})^2}{2\sigma^2} \tag{4.31}$$

we have, for $\overline{\omega}_{D^*} = \overline{\omega}_{A^*}$

$$\overline{k^2} = \bar{k}^2 \left[\frac{1 + (\sigma/\overline{\omega})^2}{2} \right] \tag{4.32}$$

$$\overline{k^4} = \bar{k}^4 \left[1 + 3\left(\frac{\sigma}{\overline{\omega}}\right)^2 + 3\frac{(\sigma/\overline{\omega})^4}{4} \right]. \tag{4.33}$$

This means that if, for instance, the ratio $\sigma/\overline{\omega}$ equals 0.1, the error made using the relationship (4.29) instead of the exact result (4.28) is less than a few percent. Furthermore, both formulas provide the corrects asymptotes at small and large distances:

1. $\bar{k}R = |n|\overline{\omega}R/c \ll 1$. Here Eqs. (4.28) and (4.29) reproduce the usual Galanin result:

$$r_1 \equiv r_1^{\text{nonrad}} = \frac{r_0}{25} \tag{4.34}$$

2. $\bar{k}R = |n|\overline{\omega}R/c \gg 1$. Here we arrive at the result for the fluorescence depolarization associated with radiative ET from the donor to an acceptor in the far zone:

$$r_1 \equiv r_1^{\text{rad}} = \frac{7r_0}{25} \tag{4.35}$$

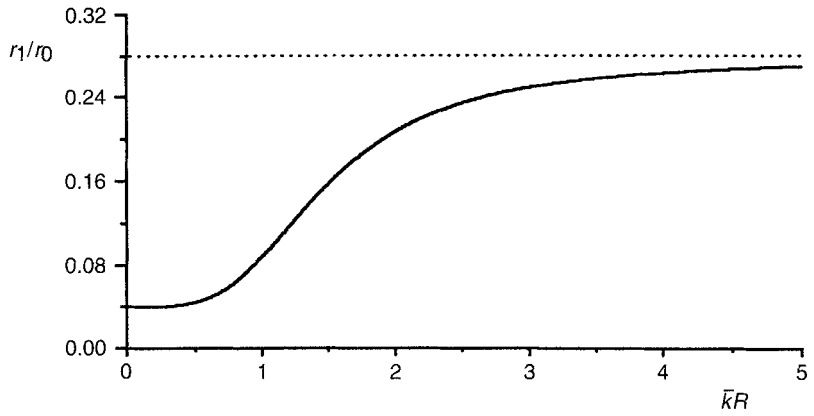

FIGURE 5. The relative anisotropy r_1/r_0 versus $\bar{k}R$ calculated according to Eq. (4.29).

The distance dependence of the relative anisotropy r_1/r_0 calculated according to Eq. (4.29) is presented in Fig. 5. One can see the anisotropy rise to significant values at distances much less than those normally associated with radiative ET. For instance, with a donor–acceptor separation $R = 1.5/\bar{k} = 0.75\lambda/\pi$, the relative anisotropy r_1/r_0 attains the value of 3/25, considerably higher than the result for radiationless transfer, as follows from Eq. (4.29). In the vacuum limit $|n| \to 1$, the results for the fluorescence anisotropy reduce to those presented in Ref. 23. In the general case ($|n| \neq 1$), the wavevector $\bar{k} = |n|\bar{\omega}/c$ is scaled by $|n|$, adjusting the characteristic scale of distances. As such, the position at which the onset of significant retardation modifies the fluorescence anisotropy can be still closer than the vacuum formula would suggest.

In connection with multiphoton fluorescence ET [117], any microscopically disordered system exhibits the same sevenfold increase in fluorescence anisotropy as the donor–acceptor distance increases from the near-zone to the far-zone range. However, the detailed dependence on the relative orientations of the participating donor transition moments adds considerable complexity to the results even in the two-photon case [117].

V. SPONTANEOUS EMISSION AS FAR-ZONE ENERGY TRANSFER

A. Background to the Problem

Spontaneous emission is a phenomenon that has played an important role in establishing several key concepts of modern quantum theory [99]. Over recent years there has been a great deal of interest in modified spontaneous

emission by atoms (molecules) in various environments, such as in photonic bandgap crystals [89–92], near metal surfaces [61–65], and near dielectric interfaces [118–121]. The characteristics of spontaneous emission are also modified in homogeneous dielectrics [72,109,110,122–128]. The rate for the process, in the case of photon emission into transparent areas of a dielectric, reads [72,109,110,125,126]*

$$W(D \leftarrow D^*) = \frac{\omega_{D^*}^3 \mu_D^2}{3\pi\varepsilon_0 \hbar c^3} n \left(\frac{n^2+2}{3} \right)^2 \tag{5.1}$$

where the transition frequency ω_{D^*} is also modified by the surrounding medium [109,126].

The emission rate (5.1) can be obtained using various methods. For instance, the explicit mode expansion (3.13) for the local operator $\mathbf{d}^{\perp}(\mathbf{R}_D)$ offers a straightforward way to derive the emission rate (5.1) [109,110] through application of the Fermi golden rule (3.1), in which the spontaneous emission appears as a first-order process described by the transition operator: $T^{(1)} = -\varepsilon_0^{-1} \boldsymbol{\mu}.\mathbf{d}^{\perp}(\mathbf{R}_D)$. The result (5.1) is relevant to the case where only long-wavelength polariton modes ($k \ll a^{-1}$) are involved in the emission process, where a is a characteristic distance between the species constituting the medium. In fact, only these modes are accommodated in the mode expansion (3.13); see the discussion following Eq. (3.17). Consequently, Eq. (5.1) does not generally hold where the emission takes place into absorbing areas of the dielectric, in which case an important role is played by excitonlike modes of the medium with larger values of k, as discussed earlier [31,109,110].

Spontaneous emission in lossy dielectrics may be considered in a number of ways. The phenomenon might be dealt with by analyzing the macroscopic Maxwell equations for a classical dipole in an absorbing medium [129]. A quantum-mechanical analysis closer in tune with the modern theoretical formalism has also been carried out [123,124]. Specifically, in a paper by Barnett et al. [124], the decay rate has been calculated for an excited atom embedded in an absorbing dielectric. Applying the Green function technique, the rate was separated into "transverse" and "longitudinal" components: these correspond, respectively, to the rate of emission of a transverse photon and the

* Equation (5.1) applies to situations where the emitting molecule does not significantly disturb the electromagnetic modes of the medium. This is known as the *virtual-cavity case* (Ref. 11, Section I.4). An alternative is the *real-cavity model*, which has been applied to spontaneous emission by Glauber and Lewenstein [122]. The latter model, introducing another local field factor into the emission rate, is relevant to situations where the emitting dipoles are large species characterised by low polarisability, such as in recent experiments by Rikken and Kessener [127] and by Schuurnams et al. [128].

rate of nonradiative decay via longitudinal coupling of the atom to the dielectric [124]. As the absorbing medium was described macroscopically, effects due to discreteness of the medium (such as the local field effects) were not intrinsically reflected; local field corrections were introduced phenomenologically at later stages [123,124]. Yet, a comprehensively microscopic approach is to be preferred.

In this section, following Refs. 31 and 73, we present a microscopic analysis of the phenomenon based on the unified approach to radiationless and radiative ET reviewed in the previous section.

B. Decay of an Excited Molecule in the Absorbing Medium

Consider the decay of an excited-state donor D induced by the transfer of energy to the surrounding species X. By summing up all appropriate pair rates, the full decay rate is

$$\Gamma_D = \sum_{X \neq D} W_{DX} \tag{5.2}$$

where W_{DX} is the rate of excitation transfer between a pair of molecules D and X, as explicitly presented in the previous section (with $X \equiv A$). Using the partition (4.12) for the pair rates, the decay rate (5.2) can be cast as

$$\Gamma_D = \tilde{\Gamma}_D^{\text{Först}} + \Gamma_D^{\text{far zone}} \tag{5.3}$$

with

$$\tilde{\Gamma}_D^{\text{Först}} = \sum_{X \neq D} (W_{DX}^{\text{Först}} + W_{DX}^{I}) \tag{5.4}$$

and

$$\Gamma_D^{\text{far zone}} = \sum_{X \neq D} W_{DX}^{\text{far zone}} \tag{5.5}$$

The former decay rate, $\tilde{\Gamma}_D^{\text{Först}}$, contains contributions due to the near-zone (Förster) pair rates modified by the intermediate terms W_{DX}^{I}; the tilde over Γ reflects such a modification. The constituent pair rates have been explicitly presented by Eqs. (4.13) and (4.15), giving the explicit refractive dependence of $\tilde{\Gamma}_D^{\text{Först}}$.

A cautionary note should be made concerning such a straightforward derivation of $\tilde{\Gamma}_D^{\text{Först}}$ in the case where most of the surrounding species X are efficient energy acceptors. In this situation, the major contribution to $\tilde{\Gamma}_D^{\text{Först}}$ comes from ET to the closest species X (up to a few configurational spheres around D). At such small distances, description of the pair rates in terms of the refractive

index is questionable. Yet, one can make use of a certain "effective" index n_{eff} in the pair rates (4.13) and (4.15) constituting the decay rate $\tilde{\Gamma}_D^{\text{Först}}$. The quantity, $n_{\text{eff}} \equiv n_{\text{eff}}(R)$, approaches the true refractive index n as the transfer distance R extends into the range where it considerably exceeds the characteristic distance between the species in the medium [11]. On the other hand, the far zone decay rate $\Gamma_D^{\text{far zone}}$ is built up of a macroscopically large number of pair rates, making its description through the refractive index quite legitimate (see discussion below). The same applies to the near-zone rate (5.4) in the case where the medium constituting the transparent background species X_1 is diluted with a small fraction of the absorbing acceptor molecules X_2. In such a case, the space between the donor and any acceptor X_2 is filled with a large number of background molecules, the latter species X_1 providing the major contribution to the refractive index n. The acceptors X_2 contribute much more weakly to n, yet ensuring the existence of some imaginary part $n'' \neq 0$ that plays an important role in the far zone through the exponential factor featured in corresponding pair rates (4.14).

In the remaining part of this section we concentrate on the decay rate $\Gamma_D^{\text{far zone}}$ associated with far-zone (radiative) ET. The far-zone transfer may be viewed [15,18,21,31,73] as spontaneous emission of a photon followed by its subsequent recapture by a distant acceptor. Adopting such a concept, we shall regard the contribution $\Gamma_D^{\text{far zone}}$ as the rate of spontaneous emission in the absorbing medium. The approach is in a certain sense related to absorber theory [130–132] in which spontaneous emission is seen to be the result of direct interaction between the emitting atom and "the Universe", the latter acting as a perfect absorber at all emitted frequencies. In our situation, the surrounding medium does indeed act as a perfect absorber even at extremely low concentrations of the absorbing species (or, alternatively, for an almost transparent condensed medium), so long as the system dimensions are large enough to ensure eventual recapture of the emitted photon. For such a weakly absorbing medium, the rate $\Gamma_D^{\text{far zone}}$ will be demonstrated to reproduce exactly the familiar rate [72,109,110,125,126] for spontaneous emission in a transparent dielectric.

To obtain the proper decay rate $\Gamma_D^{\text{far zone}}$ using Eq. (5.5), the pair-transfer rates $W_{DX}^{\text{far zone}}$ should not only reflect effects due to retardation but also incorporate influences of the surrounding medium, as in the previous section. Following Refs. 31 and 73, we shall demonstrate that $\Gamma_D^{\text{far zone}}$ does indeed represent the rate of spontaneous emission in the absorbing medium. For this purpose, we substitute Eq. (4.14) for the pair-rate $W_{DA}^{\text{far zone}}$ (with $A \equiv X$) into Eq. (5.5) to yield

$$\Gamma^{\text{far zone}} = \frac{9}{8\pi\tau_D} \int_0^\infty F_D(\omega) \sum_X R^{-2} \eta_1^2 \sigma_X(\omega) e^{-2n''\omega R/c} \mathrm{d}\omega \qquad (5.6)$$

with $\mathbf{R} \equiv \mathbf{R}_{XD}$. The decay rate $\Gamma_D^{\text{far zone}}$ is made up of a large number of the pair rates operating predominantly in the far zone. Hence the summation over the molecules X can be changed to an integral over the radius vector $\mathbf{R}$, giving

$$\Gamma^{\text{far zone}} = \frac{1}{\tau_D} \int_0^\infty \mathrm{d}\omega F_D(\omega)\sigma(\omega) \int_0^\infty \mathrm{d}R e^{-2n''\omega R/c} \tag{5.7}$$

$$= \frac{c}{2\tau_D} \int_0^\infty \mathrm{d}\omega F_D(\omega)\sigma(\omega)/\omega n'' \tag{5.8}$$

where [in Eq. (5.7)] the appropriate orientational averaging has been carried out ($[\eta_1^2 \to \langle \eta_1^2 \rangle = \frac{2}{9}]$) and the cross section of the molecular absorption $\sigma_X(\omega)$ has been replaced by its ensemble average as given by

$$\sigma(\omega) \equiv \bar{\sigma}_X(\omega) = \frac{\omega}{c}\frac{1}{n'}\left|\frac{n^2+2}{3}\right|^2 \frac{\bar{\alpha}_X''}{\varepsilon_0} \tag{5.9}$$

Here, the quantity $\bar{\alpha}_X$ is understood as an averaged polarizability for all the species X constituting the medium:

$$\bar{\alpha}_X = N^{-1} \sum_X \alpha_X \tag{5.10}$$

where N is the total number of molecules in the system. The relationship (5.9) has been written exploiting Eq. (4.9) for $\sigma_A(\omega)$ (with $A \equiv X$). Here, constraints due to the energy-conserving delta functions have been expressed in terms of the imaginary part of the averaged molecular polarizability $\bar{\alpha}_X'' \equiv \alpha''$, as given by Eq. (5.10) with

$$\alpha_X \equiv \alpha_X(\omega + is) = \frac{1}{3\hbar} \sum_{m,p} \rho_X^{(m)} \left[\frac{\mu_X^2 |\langle \varphi_{X^*}^{(p)} | \varphi_X^{(m)} \rangle|^2}{\omega_{X_{pm}^*} - \omega - is} + \frac{\mu_X^2 |\langle \varphi_{X^*}^{(p)} | \varphi_X^{(m)} \rangle|^2}{\omega_{X_{pm}^*} + \omega + is} \right] \tag{5.11}$$

and where $\omega_{X_{pm}^*} = \omega_{X_p^*} - \omega_{X_m}$ is the excitation frequency of the molecule X and $|\langle \varphi_{X^*}^{(p)} | \varphi_X^{(m)} \rangle|^2$ are the Condon factors defined in Section IV.A (with $A \equiv X$). The imaginary part α'' is in turn related to the complex refractive index $n \equiv n(\omega)$, as

$$n'' = \frac{1}{2n'}\left|\frac{n^2+2}{3}\right|^2 \frac{\alpha''\rho}{\varepsilon_0} \tag{5.12}$$

so that Eq. (5.9) ultimately reduces to

$$\sigma(\omega) \equiv \bar{\sigma}_X(\omega) = \frac{n''2\omega}{c\rho} \tag{5.13}$$

This equation can be identified as the usual relationship between the imaginary part of the complex refractive index and the absorption cross section. In this way, the quantity $\sigma(\omega)$ defined by Eq. (4.9) is indeed seen to represent the cross section of molecular absorption in the lossy medium. Substituting Eq. (5.13) into (5.8), one finds, using Eq. (4.10) for $F_D(\omega)$ and the normalization condition (4.11)

$$\Gamma^{\text{far zone}} = \tau_D^{-1} = \sum_{n,r} (\tau_D^{rn})^{-1} \rho_{D^*}^{(n)} \tag{5.14}$$

with

$$(\tau_D^{rn})^{-1} = \frac{\omega_{D^*_{nr}}^3 \mu_D^2}{3\hbar\varepsilon_0 \pi c^3} n' \left| \frac{n^2+2}{3} \right|^2 |\langle \varphi_D^{(r)} | \varphi_{D^*}^{(n)} \rangle|^2 \tag{5.15}$$

The rate $\Gamma^{\text{far zone}} = \tau_D^{-1}$ as given by Eqs. (5.14) and (5.15) represents the full rate of spontaneous emission by the donor, and so involves summation over the final levels and averaging over the initial levels of the donor, labeled respectively r and n, where $\rho_{D^*}^{(n)}$ is the population distribution of the vibrational levels of donor in the initially excited electronic state. The constituent terms $(\tau_D^{rn})^{-1}$ represent the partial rates of spontaneous emission associated with downward transitions of the donor between the specific levels n and r, where in each of these terms the refractive index is to be calculated at the appropriate emission frequency $\omega_{D^*} \equiv \omega_{D^*_{nr}} = (e_{D^*_n} - e_{D_r})/\hbar$.

The emission rates (5.15) manifestly accommodate contributions due to the absorbing dielectric medium, including the local field factors. In addition, the emission frequency ω_{D^*} is to be renormalized to include the effects of the medium, as follows from the strict analysis of ET dynamics presented in the next section. It is noteworthy that our analysis is based on a microscopic QED theory [28,31], the relationship (5.15) supporting previous phenomenological methods [123,124] used to introduce local field corrections to the rates of spontaneous emission in an absorbing medium. In the limit where $\alpha'' \to 0$, $n'' \to 0$, the far-zone rate [Eqs. (5.14) and (5.15)] reduces smoothly to the usual result for spontaneous emission in a transparent medium given by Eq. (5.1) (in which Condon factors are not included); in such a situation there is a vanishing contribution due to the decay in the near and intermediate zones: $\tilde{\Gamma}_D^{\text{Först}} \to 0$.

In this way, the present analysis reproduces in full the rate of spontaneous emission in transparent dielectrics $n'' = 0$, including, inter alia, the case of free space: $n'' = 0, n' = 1$. Here, free space is be to viewed as a limit in which the density of the absorbing species goes to zero, while the size of the system goes to infinity, so that the emitted photon is eventually recaptured somewhere in the system. It is notable that in order to arrive at a sensible result for

$\Gamma_D^{\text{far zone}} = \tau_D^{-1}$, such as that given by Eqs. (5.14) and (5.15), the influences of the absorbing medium are necessarily to be reflected in the pair-transfer rates constituting the far-zone decay rate (5.5). In fact, it is the exponential factor $\exp(-2n''\omega R/c)$, representing absorption losses at the intervening medium, that helps avoid the potentially infinite decay rate $\Gamma_D^{\text{far zone}}$ due to the R^{-2} factor featured in the constituent pair rates (4.14). Note also that the same result, (5.14) and (5.15), can be reproduced for the rate of spontaneous emission τ_D^{-1}, in terms of another microscopic method involving calculation of the quantum flow from the emitting molecule D in the absorbing medium [73].

It is noteworthy that the separation of the full decay rate into far- and near-zone components corresponds to a division of the rate into its "transverse" and "longitudinal" parts, to use the terms adopted by Barnett et al. [124]. Our description in terms of far- and near-zone rates goes along with the multipolar formulation of QED employed here; in such a formulation, [96], the coupling between the molecules is mediated exclusively via transverse photons, as there is no instantaneous (longitudinal) contribution to the intermolecular coupling. Finally, the analysis presented yields the exponential decay with time of the excited-state population for a selected molecule D, as long as the backtransfer of the excitation energy from the surrounding species X is negligible. The near-zone contribution to the decay rate, $\tilde{\Gamma}_D^{\text{Först}}$ [Eq. (5.4)], may depend markedly on a specific distribution of acceptors around the donor in the case of a somewhat inhomogeneous medium. At short times, this leads to the well-known [11] nonexponential time decay of the excited-state population averaged over the ensemble. On the other hand, the total rate of radiative ET $\Gamma_D^{\text{far zone}}$ depends much more weakly on the specific site of the emitter D, yielding an exponential contribution to the time decay of the excited-state population in the ensemble. Exponential decay dominates the kinetics at sufficiently large times.

VI. DYNAMICS OF ET BETWEEN A PAIR OF MOLECULES IN A DIELECTRIC MEDIUM

Up to now the transfer dynamics has been described in terms of well-defined rates for intermolecular ET. It is the purpose of the current section to pursue in more detail temporal aspects of the ET between a pair of species in a dielectric medium. The consideration is based on the QED study [28], a distinctive aspect of which is a combined analysis of rate- and nonrate regimes in the context of examining the influence of the dielectric medium on a microscopic basis. The theory is built on the foundation established in the previous sections. Again, the approach exploits the concept of ET mediated by bath polaritons. The theory also makes use of the microscopically derived tensor (3.18) for the retarded and medium-dressed dipole–dipole coupling, now with regard to the dynamical behavior. The present section not only extends consideration

beyond the rate description, but also reexamines conditions for that regime itself. That leads to incorporation of the shifts in energy for both the ground and excited states of the transfer species, due to the interaction of these species with the molecules belonging to the medium and also with each other. That is a feature not reflected in direct application of the ordinary Fermi golden rule.

The section is organised as follows. In the next subsection the Heitler–Ma method [2,54,95,133,134] for describing the quantum time evolution is first outlined, and subsequently reformulated to suit our current purposes. Consequently, the basic equations for time evolution acquire a form more symmetric with respect to the initial and final states. Section VI.B presents the general analysis on the transfer dynamics between a pair of molecules in the molecular medium. At the end of the Section VI.B, we discuss the problem of causality in ET, an issue that has received a great deal of interest in the literature [39–52]. Section VI.C deals with the specific situations including both the rate regime and beyond. Note that the non-rate regime features in situations lacking an intrinsic density of molecular states for the participating species.

A. Time Evolution of a Quantum System

Consider the quantum dynamics of a system with a time-independent Hamiltonian separable as the sum of a zeroth-order Hamiltonian H^0 and an interaction term V [such as that defined by Eq. (2.5)], where the eigenvectors of H^0 include both the initial state $|I\rangle$ and the final state $|F\rangle$ for the process. For reasons which will become apparent later, we shall commence work in the Schrödinger representation rather than the more common interaction representation. The state vector of the system then evolves at positive times from the state $|I\rangle$ at $t = +0$ as

$$S(t)|I\rangle = \Theta(t)e^{-iHt/\hbar}|I\rangle \tag{6.1}$$

$$= -\frac{1}{2\pi i}\int_{-\infty}^{+\infty} \mathrm{d}\varepsilon e^{-i\varepsilon t/\hbar}(\varepsilon - H + is')^{-1}|I\rangle, \qquad s' \to +0 \tag{6.2}$$

where $\Theta(t)$ is the unit step (Heaviside) function. Strictly speaking, the quantity $s' \equiv \hbar s$ is a positive infinitesimal. Yet, for finite times it may be considered a finite quantity obeying the following: $st \ll 1$, that is, s should be kept much less than the inverse lifetime for the excited states. Under this condition, introduction of a finite s does not influence the quantum dynamics governed by Eq. (6.2). Retention of a finite value for s plays an important role in smoothing of spectral lines. This makes the refractive index given by Eq. (3.19) [together with Eqs. (3.15) and (3.16)] a complex quantity in absorbing areas of the spectrum (characterized by densely spaced molecular sublevels of vibrational or other origin for each electronic transition).

The Heitler–Ma method [2,54,95,133,134] may now be employed, giving

$$\langle F|(\varepsilon - H + is')^{-1}|I\rangle = \frac{U_{FI}(\varepsilon)}{(\varepsilon - E_F + is')[\varepsilon - E_I + \frac{1}{2}i\hbar\Gamma_1(\varepsilon) + is']} \tag{6.3}$$

Here $U_{FI}(\varepsilon) \equiv \langle F|U(\varepsilon)|I\rangle$ and $\Gamma_I(\varepsilon) \equiv \langle I|\Gamma(\varepsilon)|I\rangle$ are, respectively, the matrix elements of the off-diagonal transition operator $U(\varepsilon)$ and the diagonal damping operator $\Gamma(\varepsilon)$, both determined by the following recurrence relation:

$$U(\varepsilon) - \tfrac{i}{2}\hbar\Gamma(\varepsilon) = V + V(\varepsilon - H^0 - V + is')^{-1}U(\varepsilon) \tag{6.4}$$

For the present purposes it is more convenient to represent this relation in a nonrecursive format as

$$[U(\varepsilon) - \tfrac{i}{2}\hbar\Gamma(\varepsilon)]|I\rangle = \lfloor V + VP_I(\varepsilon - H^0 - P_IVP_I + is')^{-1}P_IV\rfloor I\rangle \tag{6.5}$$

where the projection (idempotent) operator

$$P_I = 1 - |I\rangle\langle I| \tag{6.6}$$

identifies the exclusion of contributions by the initial state in the perturbation expansion of Eq. (6.5). Recasting the transition matrix element in a form where the perturbational contribution by the final state also no longer explicitly features, one arrives at (see Appendix B of Ref. 134)

$$U_{FI}(\varepsilon) = \frac{\varepsilon - E_F + is'}{\varepsilon - E_F + \frac{i}{2}\hbar\Gamma'_F + is'}U'_{FI} \tag{6.7}$$

where the newly defined quantities on the right, U'_{FI} and Γ'_F, both have implicit ε dependence and are given by

$$U'_{FI} \equiv \langle F|\lfloor V + VP_IP_F(\varepsilon - H^0 - P_IP_FVP_IP_F + is')^{-1}P_IP_FV\rfloor I\rangle \tag{6.8}$$

$$-\tfrac{i}{2}\hbar\Gamma'_F \equiv \langle F|\lfloor V + VP_IP_F(\varepsilon - H^0 - P_IP_FVP_IP_F + is')^{-1}P_IP_FV\rfloor I\rangle \tag{6.9}$$

with

$$P_F = 1 - |F\rangle\langle F| \tag{6.10}$$

Finally, calling on Eqs. (6.2), (6.3), and (6.7), one finds the following probability amplitude for the transition $|I\rangle \to |F\rangle$:

$$\langle F|S(t)|I\rangle = -\frac{1}{2\pi i}\int_{-\infty}^{+\infty} d\varepsilon \frac{U'_{FI}e^{-i\varepsilon t/\hbar}}{(\varepsilon - E_F + \frac{i}{2}\hbar\Gamma'_F + is')(\varepsilon - E_I + \frac{i}{2}\hbar\Gamma_I + is')} \tag{6.11}$$

which is an exact result. Here the presence of both Γ_I and Γ'_F in the energy denominators explicitly accommodates the damping corrections and energy renormalization of the initial and final states. Consequently, the transfer amplitude as presented above has a form obviously more symmetric with respect to the initial and final states than would result from direct substitution of Eq. (6.3) into (6.2). Still, there is some asymmetry with respect to these states, reflected by the prime on Γ'_F. The retention of such a asymmetry will be of vital importance in the case of sharp energy levels for donor and acceptor, that is, where the participating transfer species lack an intrinsic density of molecular states; this aspect is to be considered in the Section VI.C.2.

B. Dynamics of Energy Transfer

The dynamical system of interest has been defined by the Hamiltonian (2.5)–(2.7′). For the representation of resonance ET, the initial and final state vectors and their energies are considered to have the form of Eqs. (2.8) and (2.9). Because of the two-center character of the interaction operator (2.6), it is convenient to carry out the corresponding partitioning in Eqs. (6.5) and (6.9), writing

$$-\tfrac{i}{2}\hbar\Gamma_I = \Delta e_{D^*} + \Delta e_A - \tfrac{i}{2}\hbar\gamma_{D^*} - \tfrac{i}{2}\hbar\Gamma_{D^*A} \tag{6.12}$$

$$-\tfrac{i}{2}\hbar\Gamma'_F = \Delta e_D + \Delta e_{A^*} - \tfrac{i}{2}\hbar\gamma_{A^*} - \tfrac{i}{2}\hbar\Gamma'_{DA^*} \tag{6.13}$$

Here one-center contributions, denoted by a single index D (or A), are due to the terms containing only one operator V_D (or V_A) in the perturbation expansions of Eqs. (6.5) and (6.9). Such contributions have already been separated into real energy shifts and imaginary damping terms in the preceding equations. For instance, Δe_{D^*} and γ_{D^*} represent, respectively, the bath-induced level shift (energy renormalization) and the damping factor for the excited molecular state $|D^*\rangle$ (as there are no imaginary (damping) contributions for the ground molecular states $|D\rangle$ and $|A\rangle$). Each such energy renormalization (Δe_{D^*}, Δe_A, Δe_D, and Δe_{A^*}) embodies not only the radiative (Lamb) shift [94–96,99] but also the contribution due to the dispersion interaction between the donor D (or acceptor A) and the molecular medium. Note that the dispersion energy appears now in the second order of perturbation, rather than the usual fourth order [94–96,135], since the coupling of the radiation field with the medium has already been included in the zero-order Hamiltonian H^0 given by Eqs. (2.7) and (2.7′). Here we do not consider the explicit structure of these energy shifts, which are to be treated as the parameters of the theory. The remaining (complex) quantities Γ_{D^*A} and Γ'_{DA^*} are two-center contributions resulting from cross-terms (containing both V_D and V_A) that emerge in the perturbation expansions of Eqs. (6.5) and (6.9).

By making use of Eqs. (6.12) and (6.13), the probability amplitude (6.11) for the ET takes the form

$$\langle F|\tilde{S}(t)|I\rangle = -\frac{1}{2\pi i\hbar}\int_{-\infty}^{+\infty} d\omega \frac{U'_{FI}(\omega)e^{-i(\omega-\omega_{A^*})t}}{(\omega-\omega_{A^*}+(i/2)\gamma_{A^*}+(i/2)\Gamma'_{DA^*}+is)(\omega-\omega_{D^*}+(i/2)\gamma_{D^*}+(i/2)\Gamma_{D^*A}+is)} \tag{6.14}$$

where

$$\omega = \frac{\varepsilon - e_D - e_A - \Delta e_D - \Delta e_A - e_{\text{vac}}}{\hbar} \tag{6.15}$$

is a new variable, and

$$\omega_{D^*} = \frac{e_{D^*} + \Delta e_{D^*} - e_D - \Delta e_D}{\hbar} \tag{6.16}$$

$$\omega_{A^*} = \frac{e_{A^*} + \Delta e_{A^*} - e_A - \Delta e_A}{\hbar} \tag{6.17}$$

are the excitation frequencies of the donor and the acceptor. The frequencies ω_{D^*} and ω_{A^*} incorporate level shifts for both the ground and excited molecular states. Finally, in Eq. (6.14) transformation has been carried out to a modified interaction representation, as

$$\langle F|\tilde{S}(t)|I\rangle = \langle F|S(t)|I\rangle \exp\frac{-i(E_F+\Delta E_F)t}{\hbar} \tag{6.18}$$

where the term "modified" refers to change of the final-state energy $E_F = e_D + e_{A^*}$ by the amount $\Delta E_F = \Delta e_D + \Delta e_{A^*}$.

Now we turn our attention to the transition matrix element $U'_{FI}(\omega)$ featured in Eq. (6.14). For the present purposes it is sufficient to represent it through an effective second-order contribution as

$$U'_{FI}(\omega) \approx U^{(2)}_{FI}(\omega) = \mu^{\text{full}}_{A_l}\theta'_{lj}(\omega, \mathbf{R})\mu^{\text{full}}_{D_j} \tag{6.19}$$

with

$$\theta_{lj}(\omega, \mathbf{R}) = \frac{1}{\hbar\varepsilon_0^2}\sum_{\sigma}\left[\frac{\langle 0|\mathrm{d}_l^{\perp}(\mathbf{R}_A)|\sigma\rangle\langle\sigma|d_j^{\perp}(\mathbf{R}_D)|0\rangle}{\omega - \Pi_\sigma + is} + \frac{\langle 0|\mathrm{d}_j^{\perp}(\mathbf{R}_D)|\sigma\rangle\langle\sigma|d_l^{\perp}(\mathbf{R}_A)|0\rangle}{\omega - \omega_{D^*} - \omega_{A^*} - \Pi_\sigma + is}\right] \tag{6.20}$$

($\mathbf{R} = \mathbf{R}_A - \mathbf{R}_D$), where implied summation over the repeated Cartesian indices (l and j) is assumed, and μ_D^{full} and μ_A^{full} are the transition dipoles given by Eq. (2.19). As in the previous sections, here $\hbar\Pi_\sigma = e_\sigma - e_{\text{vac}}$ is the excitation energy of the bath, the index σ denoting excited (single polariton) states of the bath accessible from the ground state $|0\rangle$ by single action of the local

displacement operator $\mathbf{d}^{\perp}(\mathbf{R}_X)(X = D, A)$. In what follows we replace the energy denominator $(\omega - \omega_{D^*} - \omega_{A^*} - \Pi_\sigma + is)$ by $(-\omega - \Pi_\sigma + is)$ in the nonresonant term of Eq. (6.20). The approximation holds for the range of frequencies $|\omega - \omega_{D^*}|$, $|\omega - \omega_{A^*}| \ll \omega_{D^*}$. Such a frequency range yields the major contribution to the integral (6.14) for times greater than the inverse molecular transition frequency $\omega_{D^*}^{-1}$, generally on the femtosecond timescale. This leads the causal result, as discussed later. Adopting the resonance approximation, the tensor $\theta'_{lj}(\omega, \mathbf{R})$ reduces to the familiar tensor for the retarded dipole–dipole coupling in the medium:

$$\theta'_{lj}(\omega, \mathbf{R}) \approx \theta_{lj}(\omega, \mathbf{R}) \tag{6.21}$$

The latter $\theta_{lj}(\omega, \mathbf{R})$ reads explicitly, using Eqs. (3.18) and (3.6)

$$\theta_{lj}(\omega, \mathbf{R}) = n\left(\frac{n^2+2}{3}\right)^2 \frac{\omega^3 e^{in\omega R/c}}{4\pi c^3 \varepsilon_0}\left[(\delta_{ij} - 3\hat{R}_i\hat{R}_j)\left(\frac{c^3}{n^3\omega^3R^3} - \frac{ic^2}{n^2\omega^2R^2}\right)\right.$$
$$\left. - (\delta_{ij} - \hat{R}_i\hat{R}_j)\frac{c}{n\omega R}\right] \tag{6.22}$$

where n is the complex relative index given by Eqs. (3.19), (3.15), and (3.16).

It is noteworthy that the quantity $U_{FI}^{(2)}(\omega_{A^*})$ is equivalent to the transition matrix element $\langle F|T^{(2)}|I\rangle$ introduced earlier by Eq. (2.17):

$$\langle F|T^{(2)}|I\rangle \equiv U_{FI}^{(2)}(\omega_{A^*}) \tag{6.23}$$

In the context of time evolution, it is important to retain the ω dependence featured in the exponential phase factor $\exp(in\omega R/c)$ of the matrix element $U_{FI}^{(2)}(\omega)$ given by Eqs. (6.19), (6.21), and (6.22). This will lead to appearance of a time lag in the initial arrival of the excitation at the acceptor A, due to the finite speed of signal propagation. Linearizing the exponent, one has

$$\frac{n(\omega)\omega R}{c} \approx \frac{n(\omega_{A^*})\omega_{A^*}R}{c} + \frac{(\omega - \omega_{A^*})R}{v_g} \tag{6.24}$$

where v_g is the radiative group velocity, given by

$$\frac{1}{v_g} = \frac{\mathrm{d}}{\mathrm{d}\omega}\left(\frac{n\omega}{c}\right)\Big|_{\omega=\omega_{A^*}} \tag{6.25}$$

The remainder of the transition element $U_{FI}^{(2)}(\omega)$, together with other ω-dependent parameters entering Eq. (6.14), will at this stage be evaluated

at the resonant frequency, $\omega = \omega_{A^*} \approx \omega_{D^*}$. Redefining the origin of time $\tau = (t - R/v_g)$, the transfer amplitude (6.14) takes the form

$$\langle F|\tilde{S}(t)|I\rangle = -\frac{1}{2\pi\hbar i}\int_{-\infty}^{+\infty} d\omega \frac{U_{FI}^{(2)}(\omega_{A^*})e^{-i(\omega-\omega_{A^*})\tau}}{(\omega - \omega_{A^*} + \frac{i}{2}\gamma_{A^*} + is)(\omega - \omega_{D^*} + \frac{i}{2}\gamma_{D^*} + is)} \tag{6.26}$$

$$= \hbar^{-1}U_{FI}^{(2)}(\omega_{A^*})\Theta(\tau)\frac{e^{-\frac{1}{2}\gamma_{A^*}\tau} - e^{\left[-\frac{1}{2}\gamma_{D^*}+i(\omega_{A^*}-\omega_{D^*})\right]\tau}}{(\omega_{A^*} - \omega_{D^*}) + \frac{1}{2}i(\gamma_{D^*} - \gamma_{A^*})} \tag{6.27}$$

which incorporates damping for both species D and A. Here the two-center contributions Γ_{D^*A} and Γ'_{DA^*} are for the present omitted; the physical basis of this approximation is clarified in Section VI.C.

It is worth noting that the radiative group velocity v_g introducing the shift of the origin of time in Eq. (6.27) describes the delay of the initial arrival of the excitation at acceptor A. On the other hand, the phase velocity $v_\phi = c/n$ entering the exponential factor $\exp(in\omega R/c)$ of the transition matrix element $U_{FI}^{(2)}(\omega_{A^*})$ [with $n \equiv n(\omega_{A^*})$] characterizes the changes of optical phase with distance. Note also that incorporation of the time lag in the manner described above implies that the refractive index, and hence also the group velocity, takes real values. Nonetheless, the general result to follow (6.28) for the transfer rates holds for both lossless and absorbing media.

In the case of ET in vacuum ($n = 1$), the acceptor can be excited only after a relativistic time delay of R/c. A similar causal conclusion has been reached already by Fermi [1], Heitler and Ma [2], and Hamilton [3]. However, removing the approximation (6.21) leading to Eq. (6.27), one would arrive at a small (yet finite) probability for the acceptor to be excited at $t < R/c$. Such a noncausal behavior has received a great deal of interest in the literature [25,39–52]. It was pointed out [40,45,50] that the causality can be restored examining the problem within a wider framework. In fact, adopting Eq. (2.8), one specifies completely the final state in which, besides to acceptor being excited, the donor is specified to be in the ground state and the field in its vacuum state at time t. To eliminate this restriction, Power and Thirunamachandran [50] and Berman and Dubetsky [51] calculated (up to terms that depend on the square of the transition moment of the emitter and the square of the moment of the receiver) the probability of the receiver atom (acceptor) being excited at time t without making any reference to the final states for both the emitter atom (donor) and the field.* For this purpose, a set of final

* This is also implicit in the studies [48,49] focusing on the time evolution of the occupation operators.

states has been extended to include the ones that are not in resonance with the initial state, such as the states where both acceptor and donor are excited, and the field is in the arbitrary state. It was found [50,51] that apart from a small R-independent term, the total probability becomes causal, that is, is identically equal to zero for $t < R/c$.

The existence of some (R-independent) probability for the acceptor to be excited at $t < R/c$, goes along with the Hegerfeldt theorem [46] stating that the initially unexcited atom (acceptor) starts to move out of the ground state immediately. As pointed out by Milonni and co-authors [49]:

The theorem as proved applies *regardless of whether ... (the emitter) is present* and therefore ... should not be used as an argument against causality in the two-atom interaction. Such "immediate influences" are associated with the fact that the assumed initial state is not an eigenstate of the interacting atom-field system: a true eigenstate of the system involves an *admixture* of "bare" states .... Such admixtures involving excited, unperturbed atomic (and field) states occur even in the case of a *single* atom coupled to the field and are associated with phenomena, such as the Lamb shift, involving virtual transitions.

C. Specific Situations

1. Rate Description

Let us consider first the case where the spectral widths of the species participating in the transfer exceed the magnitude of the corresponding transition matrix elements. The overall migration is then incoherent, described as a multistep process involving uncorrelated events of excitation transfer between the molecules of the system. In terms of the selected pair DA, by omitting the relaxation terms γ_{D^*} and γ_{A^*} in Eq. (6.27), and for times in excess of the transmit time R/v_g, the resultant rate of the excitation transfer reads

$$W_{FI} = \frac{\mathrm{d}}{\mathrm{d}t}|\langle F|\tilde{S}(t)|I\rangle|^2 = \frac{2\pi}{\hbar}|U_{FI}^{(2)}(\omega_{D^*})|^2\delta(\hbar\omega_{D^*} - \hbar\omega_{A^*}) \tag{6.28}$$

This provides the Fermi golden rule exploited previously, subject to the replacement of $U_{FI}^{(2)}(\omega_{A^*})$ by $\langle F|T^{(2)}|I\rangle$ using the relationship (6.23). The full pair-transfer rate W_{DA} is subsequently obtained by means of the standard procedure involving averaging over initial and summing over final molecular sublevels, as in the previous sections.

A new feature arising in the present dynamical analysis is that the excitation frequencies ω_{D^*} and ω_{A^*} are shifted by the interaction of the transfer species D and A with the molecules of the surrounding medium. The mutual interaction of D with A may also be taken into account by retaining the omitted terms Γ_{D^*A} and Γ'_{DA^*} in Eq. (6.26). This introduces additional shifts of the molecular

excitation frequencies ω_{D^*} and ω_{A^*} featured in the energy-conservation δ function of Eq. (6.28), by the amounts $-\mathrm{Im}\Gamma_{D^*A}/2$ and $-\mathrm{Im}\Gamma'_{DA^*}/2$, respectively: these represent changes in the excitation energy of each transfer species due to its interaction with the other. The effects of such corrections decrease with distance; over the separations of interest where R is greater than typical intermolecular distances within the medium, they can contribute negligibly.

At this juncture, a remark should be made concerning some asymmetry of the formalism with regard to the initial and final states, as reflected by the prime on Γ'_{DA^*}. The rate regime generally implies the existence of a dense structure of (usually vibrational) molecular energy levels within the electronic manifolds of D and A. Hence the apparent asymmetry in question vanishes, as either inclusion or exclusion of the individual states (such as $|I\rangle$ or $|F\rangle$) in the intermediate-state summation does not significantly alter the quantities Γ_{D^*A} and Γ'_{DA^*}. It is a different story in the case where there is no intrinsic density of molecular states for the participating species, as is to be considered next.

2. *Nonrate Regime*

Suppose now that each of the ground- and exited-state manifolds of D and A is characterized by only one molecular sublevel, so that the subsystem DA may be treated as a pair of two-level species. Ignoring contributions from states with two or more mediating bath excitations (polaritons), the exchange of energy between D and A now occurs exclusively through intermediate states in which both transfer species are in either their ground or excited states, and the bath is in a one-polariton excited state. Under these conditions, the quantities Γ_{D^*A} and Γ'_{DA^*} introduced in Eqs. (6.12) and (6.13) are

$$-\tfrac{i}{2}\Gamma_{D^*A} = \frac{[U_{FI}^{(2)}(\omega)]^2/\hbar^2}{\omega - \omega_{A^*} + \frac{i}{2}\gamma_{A^*} + is} \tag{6.29}$$

$$\Gamma'_{DA^*} = 0 \tag{6.30}$$

where use has been made of Eqs. (6.5) and (6.9). Substituting these results for Γ'_{DA^*} and Γ_{D^*A} into the general dynamical equation (6.14), the probability amplitude reads

$$\langle F|\tilde{S}(t)|I\rangle = -\tfrac{1}{2\pi\hbar i}\int_{-\infty}^{+\infty} \mathrm{d}\omega \times \frac{U_{FI}^{(2)}(\omega)e^{-i(\omega-\omega_{A^*})t}}{(\omega - \omega_{A^*} + \frac{i}{2}\gamma_{A^*} + is)(\omega - \omega_{D^*} + \frac{i}{2}\gamma_{D^*} + is) - [U_{FI}^{(2)}(\omega)/\hbar]^2} \tag{6.31}$$

To illustrate the precise form of the time evolution for a specific application, we assume the transfer species to be identical ($\omega_{D^*} = \omega_{A^*}$, $\gamma_{D^*} = \gamma_{A^*}$). Furthermore, we replace $U_{FI}^{(2)}(\omega)$ by its resonant value $U_{FI}^{(2)}(\omega_{D^*})$ in Eq. (6.31). In so doing we neglect the relativistic delay in exchanging the excitation between the donor and acceptor,* giving

$$|\langle F|\tilde{S}(t)|I\rangle|^2 = \tfrac{1}{2}[\cosh(\gamma_{DA}t) - \cos(2\Omega_{DA}t)]e^{-\gamma_{D^*}t} \tag{6.32}$$

where the transfer frequency Ω_{DA} and the inverse time γ_{DA} respectively represent the real and imaginary parts of the transition matrix element calculated at the transfer frequency

$$\hbar^{-1}U_{FI}^{(2)}(\omega_{D^*}) = \Omega_{DA} - \tfrac{i}{2}\gamma_{DA} \tag{6.33}$$

Equation (6.32) has a form familiar from the case of ET between molecules in vacuo [34,53–55], although the parameters γ_{DA}, γ_{A^*}, and Ω_{DA} here display the influence of the medium. The result for nonidentical species in vacuum is presented in Ref. 55. Note that although in writing Eqs. (6.29)–(6.33) the transfer species D and A have been modeled as two-level systems, the formulation still allows each surrounding molecule to possess an arbitrary number of energy levels, thus accommodating the cases of both absorbing and lossless media.

The result (6.32) represents an oscillatory, to-and-fro exchange of excitation, accompanied by damping. That type of dynamical behavior is a direct consequence of the absence of a density of final molecular states, a feature that obviously makes the rate description inadequate. Nonetheless, a distinction should be drawn between the short-range reversible Rabi-type oscillatory behavior, which does not represent any real flow of energy from D to A, and the long-range behavior. In the latter case, the excitation energy of the donor is irreversibly passed to the acceptor. Under such circumstances it is appropriate to introduce transfer probabilities (rather than rates), as shown in the remaining part of this section.

In the long-range limit, the contribution $[U_{FI}^{(2)}]^2$ associated with the coupling between the donor and the acceptor may legitimately be omitted in the denominator of the integrand in Eq. (6.31), in which D and A are not necessarily identical two-level species. The system then follows the same time evolution as described through the earlier equation [Eq. (6.27)]. The transfer

* Such a time delay leading to the effects of multiple time delay in to-and-fro exchange of excitation, has been investigated by Milonni and Knight [36], who analyzed the transfer dynamics between a pair of species in vacuo.

dynamics governed by Eq. (6.27) reflects both the initial arrival of excitation at A, commencing from time $t = R/v_g$, and subsequent decay of the resulting excited state of the acceptor.* The rate of the latter decay may be considered to be the same as that for an individual acceptor in the dielectric medium (i.e., γ_{A^*}), since at large distances the remaining influence of the donor is minimum. Accordingly, the total transfer probability P may be defined as the probability for irreversible trapping of the excitation by the acceptor. Integrating the population-weighted rate of decay of the excited state of A, one finds

$$P = \int_{R/v_g}^{\infty} |\langle F|\tilde{S}(t)|I\rangle|^2 \gamma_{A^*} \mathrm{d}t \tag{6.34}$$

$$= (\Omega_{DA}^2 + \gamma_{DA}^2)\gamma_{D^*}^{-1} \frac{(\gamma_{D^*} + \gamma_{A^*})}{(\omega_{A^*} - \omega_{D^*})^2 + (\gamma_{D^*} + \gamma_{A^*})^2/4} \tag{6.35}$$

which is in agreement with the previous far-zone result for the transfer of energy between a pair of molecules in vacuo [37]. In passing we note that the individual rates of the excited-state decay $\gamma_{D^*} \equiv \Gamma_D$ and $\gamma_{A^*} \equiv \Gamma_A$ featured in the above equations have been explicitly analyzed in the Section V.B. Calling on Eqs. (6.19), (6.21), (6.22), and (6.33), the long-range result (6.35) assumes the following form in the case of a nonabsorbing medium:

$$P = \frac{9}{8\pi} \langle \sigma_A \rangle \frac{[(\hat{\mu}_D \cdot \hat{\mu}_A) - (\hat{\mu}_D \cdot \hat{\mathbf{R}})(\hat{\mu}_A \cdot \hat{\mathbf{R}})]^2}{R^2} \tag{6.36}$$

with

$$\langle \sigma_A \rangle = \frac{1}{n} \left(\frac{n^2 + 2}{3} \right)^2 \frac{\mu_A^2 \omega_{A^*}}{3\varepsilon_0 \hbar c} \left[\frac{(\gamma_{D^*} + \gamma_{A^*})/2}{(\omega_{A^*} - \omega_{D^*})^2 + (\gamma_{D^*} + \gamma_{A^*})^2/4} \right] \tag{6.37}$$

Here, in addition to the appearance of the refractive prefactors, the influence of the medium extends to the excitation frequencies ω_{D^*} and ω_{A^*}, as well as to the decay parameters γ_{A^*} and γ_{B^*}. The quantity $\langle \sigma_A \rangle$ may be identified as the isotropic absorption cross section of acceptor, $\sigma_A(\omega)$, averaged over the normalized emission spectrum of donor, $I_{D^*}(\omega)$, as:

$$\langle \sigma_A \rangle = \int_{-\infty}^{+\infty} \sigma_A(\omega) I_{D^*}(\omega) \mathrm{d}\omega \tag{6.38}$$

---

* For a particular case involving two identical species D and A, the probability for the acceptor to be excited is represented by an initial waiting interval $t = R/c$, followed by a quadratic rise time and subsequent exponential decay, in accordance with the classical wave-zone result in vacuo by Hamilton [3].

with $\sigma_A(\omega)$ and $I_{D^*}(\omega)$ given by

$$\sigma_A(\omega) = \frac{1}{n}\left(\frac{n^2+2}{3}\right)^2 \frac{\mu_A^2 \omega_{A^*}}{3\varepsilon_0 \hbar c}\left[\frac{\gamma_{A^*}/2}{(\omega-\omega_{A^*})^2+(\gamma_{A^*}/2)^2}\right] \tag{6.39}$$

and

$$I_{D^*}(\omega) = \frac{1}{\pi}\left[\frac{\gamma_{D^*}/2}{(\omega-\omega_{D^*})^2+(\gamma_{D^*}/2)^2}\right] \tag{6.40}$$

Finally, one obtains, for the orientationally averaged probability

$$\overline{P} = \frac{\langle \sigma_A \rangle}{4\pi R^2} \tag{6.41}$$

which is the ratio of the spectrally averaged isotropic absorption cross section to the spherical surface at distance R, $4\pi R^2$. In the case of an absorbing medium, an exponential decay factor of the form $\exp(-2n''\omega R/c)$ would also feature in this equation.

Throughout this section, the transition matrix element U'_{FI} (as well as the damping quantities Γ_I and Γ'_F) have been considered to be relatively smooth functions of frequency ω. Such an assumption holds well for the ET in vacuum and in the dielectric media (away from the sharp resonances). The approximation breaks down near the bandgaps or other singularities of the photon spectra. Analysis of the temporal behavior of excitation exchange between a pair of atoms in high-Q cavities [77,87] and in photonic bandgap crystals [77] has been carried out recently using different methods. Such a unusual dynamics can be treated using the present methods as well by including the ω dependence of the quantities U'_{FI}, Γ_I, and Γ'_F featured in Eq. (6.11). However, this goes beyond the scope of the present review.

VII. CONCLUSION

The chapter reviews the QED theories on the resonance energy transfer (ET) in the free space (electromagnetic vacuum), in photonic bandgap crystals, and in dielectric media. Following the general analysis, the review concentrates on the ET taking place in dielectric media, a specific example of which is free space. The formalism is based on the explicit consideration of the quantized radiation field coupled to a discrete molecular medium, where the constituent molecules of the latter are characterized by an arbitrary number of excitation frequencies. Accordingly, the ET appears to be mediated by photons "dressed" by the medium (virtual polaritons). Rates have been derived for the ET between a pair of species: donor and acceptor. The pair-transfer rates connect and accommodate both the nonradiative (Förster) R^{-6} result and also the radiative

R^{-2} result. Subsequently the range dependence of the polarization of acceptor fluorescence has been considered, the result exhibiting an interplay between the radiationless and the radiative behavior.

The microscopically derived pair-transfer rates contain the refractive contributions, including inter alia the local field factors. In the absorbing areas of the spectrum, the pair-transfer rates embody the exponential (Beer law) decay factor as well. This makes it possible to avoid the problem of potentially infinite total rates of the ET in an ensemble, due to the far-zone R^{-2} factor featured in the pair-transfer rates. By summing up the constituent far-zone rates, one arrives at the rate of the spontaneous emission in the absorbing medium containing the proper local field factors. The result supports the previous phenomenological methods used to introduce local field corrections to the rates of spontaneous emission in absorbing media. Finally, the temporal aspects of the ET have been considered. A combined analysis of rate and nonrate regimes has been presented taking into account the influence of the dielectric medium on a microscopic basis. The problem of causality in the ET is also discussed.

APPENDIX A. OPERATOR FOR THE LOCAL DISPLACEMENT FIELD

In this appendix, we derive the mode expansion of the operator $\mathbf{d}^{\perp}(\mathbf{R}_X)$. The derivation is similar to that presented in Ref. 111. We demonstrate that the expansion (3.13) represents the local displacement field calculated either at a lattice site, or at an intersitial location.

Consider the operator for the displacement field at a yet unspecified site $\mathbf{R_X}$:

$$\mathbf{d}^{\perp}(\mathbf{R}_X) = \varepsilon_0 \mathbf{e}^{\perp}(\mathbf{R}_X) + \mathbf{p}^{\perp}(\mathbf{R}_X) \tag{A.1}$$

where the mode expansion of the microscopic transverse polarization field is given by [111]

$$\mathbf{p}^{\perp}(\mathbf{R}_X) = i \sum_{\mathbf{k},\mathbf{G}} \sum_{m} \sum_{\lambda=1}^{2} \left(\frac{\varepsilon_0 \hbar \omega_k^{(m)} v_g^{(m)}}{2cV_0 n(\omega_k^{(m)})} \right)^{1/2} \{[n(\omega_k^{(m)})]^2 - 1\}$$
$$\times \mathbf{g}^{(\lambda)}(\mathbf{k}, \mathbf{G})(e^{i(\mathbf{k}+\mathbf{G}).\mathbf{R}_X} P_{\mathbf{k},m,\lambda} - e^{-i(\mathbf{k}+\mathbf{G}).\mathbf{R}_X} P^{+}_{\mathbf{k},m,\lambda}) \tag{A.2}$$

(for $k \ll 2\pi/a$), with

$$\mathbf{g}^{(\lambda)}(\mathbf{k}, \mathbf{G}) = \sum_{\lambda_1=1}^{2} \mathbf{e}^{(\lambda_1)}(\mathbf{k}+\mathbf{G})[\mathbf{e}^{(\lambda_1)}(\mathbf{k}+\mathbf{G}).\mathbf{e}^{(\lambda)}(\mathbf{k})] \tag{A.3}$$

where $\mathbf{G}$ is an inverse lattice vector. Equation (A.2) can be rewritten as

$$\mathbf{p}^{\perp}(\mathbf{R}_X) = i \sum_{\mathbf{k}} \sum_{m} \sum_{\lambda=1}^{2} \left(\frac{\varepsilon_0 \hbar \omega_k^{(m)} v_g^{(m)}}{2cV_0 n(\omega_k^{(m)})} \right)^{1/2} \{[n(\omega_k^{(m)})]^2 - 1\}$$
$$\times [\mathbf{A}^{(\lambda)+}(\mathbf{k}) P_{\mathbf{k},m,\lambda} - \mathbf{A}^{(\lambda)-}(\mathbf{k}) P^{+}_{\mathbf{k},m,\lambda}] \tag{A.4}$$

with

$$\mathbf{A}^{(\lambda)\pm}(\mathbf{k}) = \sum_{\mathbf{G}} \mathbf{g}^{(\lambda)}(\mathbf{k}, \mathbf{G}) e^{\pm i(\mathbf{k}+\mathbf{G}).\mathbf{R}_X} \tag{A.5}$$

Performing summation over λ_1 in $\mathbf{g}^{(\lambda)}(\mathbf{k}, \mathbf{G})$, one has, for the Cartesian components of $\mathbf{A}^{(\lambda)\pm}(\mathbf{k})$

$$A_j^{(\lambda)\pm}(\mathbf{k}) = \sum_{p=1}^{3} e_p^{(\lambda)}(\mathbf{k}) \sum_{\mathbf{G}} f_{jp}(\mathbf{k}+\mathbf{G}) e^{\pm i(\mathbf{k}+\mathbf{G}).\mathbf{R}_X} \tag{A.6}$$

where

$$f_{jp}(\mathbf{k}') = (\tfrac{1}{3}\delta_{jp} - \hat{k}_j \hat{k}_p) + \tfrac{2}{3}\delta_{jp} \tag{A.7}$$

and $\hat{\mathbf{k}}' \equiv \mathbf{k}'/k'$. The sum over the inverse lattice can be represented as

$$\sum_{\mathbf{G}} f_{jp}(\mathbf{k}+\mathbf{G}) e^{\pm i(\mathbf{k}+\mathbf{G}).\mathbf{R}_X} = \frac{1}{N} \sum_{\mathbf{r}_{\zeta'}} \left[\sum_{\mathbf{k}'} f_{jp}(\mathbf{k}') e^{i\mathbf{k}'.(\mathbf{r}_{\zeta'} \pm \mathbf{R}_X)} \right]$$
$$e^{-i\mathbf{k}.(\mathbf{r}_{\zeta'} \pm \mathbf{R}_X)} e^{\pm i\mathbf{k}.\mathbf{R}_X} \tag{A.8}$$

where $\mathbf{k}'$ is no longer restricted to the first Brillouin zone, as the summation over $\mathbf{r}_{\zeta'}$ covers all N sites of a periodic cubic lattice. The sum over $\mathbf{k}'$ in the square brackets can be identified as the tensor for the dipole–dipole coupling at a distance $\mathbf{r}_{\zeta'} \pm \mathbf{R}_X$, the whole of Eq. (A.8) representing the familiar dipole sum [136,137]. If $\mathbf{R}_X$ belongs to a lattice site, the term with $\mathbf{r}_{\zeta'} \pm \mathbf{R}_X = 0$ is to be excluded from Eq. (A.8), as this contribution describes an infinite self-field.

Consider the local field operator at either a lattice site $\mathbf{R}_X = \mathbf{r}_{\zeta''}$ or an intersitial location $\mathbf{R}_X = \mathbf{r}_{\zeta''} + (\mathbf{e}_1 + \mathbf{e}_2 + \mathbf{e}_3)a/2$, where $\mathbf{e}_j$ is a unit Cartesian vector. In such a situation, the terms with $\mathbf{r}_{\zeta'} = \mathbf{r}_{\zeta}$ and $\mathbf{r}_{\zeta'} = -\mathbf{r}_{\zeta} \mp 2\mathbf{R}_X$ compensate each other at small distances $\mathbf{r}_{\zeta'} \pm \mathbf{R}_X$ in Eq. (A.8). The sum over $\mathbf{r}_{\zeta'}$ may then be replaced by an integral in Eq. (A.8), so that one finds, from the resultant double Fourier integral

$$\sum_{\mathbf{G}} f_{jp}(\mathbf{k}+\mathbf{G}) e^{\pm i(\mathbf{k}+\mathbf{G}).\mathbf{R}_X} = \left(\frac{1}{3}\delta_{jp} - \hat{k}_j \hat{k}_p \right) e^{\pm i\mathbf{k}.\mathbf{R}_X} \tag{A.9}$$

Here the contribution from the second term of Eq. (A.7) has been excluded, as this term generates a δ function at $\mathbf{r}_{\zeta'} \pm \mathbf{R}_X = 0$. Since $\mathbf{e}^{(\lambda)}(\mathbf{k}) \perp \mathbf{k}$ for $\lambda = 1, 2$, substituting Eq. (A.9) into (A.6), one arrives at

$$\mathbf{A}_j^{(\lambda)}(\mathbf{k}) = \tfrac{1}{3}\mathbf{e}^{(\lambda)}(\mathbf{k}) \tag{A.10}$$

This equation, together with Eq. (A.4), leads to

$$\mathbf{p}^{\perp}(\mathbf{R}_X) = \tfrac{1}{3}\bar{\mathbf{p}}^{\perp}(\mathbf{R}_X) = \frac{i}{3}\sum_{\mathbf{k}}\sum_{m}\sum_{\lambda=1}^{2}\left(\frac{\varepsilon_0\hbar\omega_k^{(m)}v_g^{(m)}}{2cV_0 n(\omega_k^{(m)})}\right)^{1/2}$$
$$[[n(\omega_k^{(m)})]^2 - 1]\mathbf{e}^{(\lambda)}(\mathbf{k})(e^{i\mathbf{k}\cdot\mathbf{R}_X}P_{\mathbf{k},m,\lambda} - e^{-i\mathbf{k}\cdot\mathbf{R}_X}P_{\mathbf{k},m,\lambda}^{+}) \tag{A.11}$$

where $\bar{\mathbf{p}}^{\perp}(\mathbf{R}_X)$ is the transverse part of the operator for the averaged (macroscopic) polarization field. Furthermore, since [111]

$$\mathbf{e}^{\perp}(\mathbf{R}_X) = \bar{\mathbf{e}}^{\perp}(\mathbf{R}_X) = i\sum_{\mathbf{k}}\sum_{m}\sum_{\lambda=1}^{2}\left(\frac{\hbar\omega_k^{(m)}v_g^{(m)}}{2\varepsilon_0 cV_0 n(\omega_k^{(m)})}\right)^{1/2}$$
$$\mathbf{e}^{(\lambda)}(\mathbf{k})(e^{i\mathbf{k}\cdot\mathbf{R}_X}P_{\mathbf{k},m,\lambda} - e^{-i\mathbf{k}\cdot\mathbf{R}_X}P_{\mathbf{k},m,\lambda}^{+}) \tag{A.12}$$

the relationships (A.1), (A.11), and (A.12) yield the required mode expansion (3.13) of the operator for the local displacement field.

APPENDIX B. CALCULATION OF THE TENSOR $\theta_{lJ}(w, \mathbf{R})$ FOR THE RETARDED RDDI IN A DIELECTRIC MEDIUM*

Calling on the mode expansion (3.13) for the local operator $\mathbf{d}^{\perp}(\mathbf{R}_X)$ (with $X = D, A$) in a dielectric medium, the RDDI tensor (2.19) takes the form

$$\theta_{lj}(\omega, \mathbf{R}) = -\frac{1}{2V_0 c\varepsilon_0}\sum_{\mathbf{k},m}\left(\frac{\omega_k^{(m)}v_g^{(m)}}{n(\omega_k^{(m)})}\right)\left[\frac{[n(\omega_k^{(m)})]^2 + 2}{3}\right]^2(\delta_{lj} - \hat{k}_l\hat{k}_j)$$
$$\times\left[\frac{e^{i\mathbf{k}\cdot\mathbf{R}}}{\omega_k^{(m)} - \omega - is} + \frac{e^{-i\mathbf{k}\cdot\mathbf{R}}}{\omega_k^{(m)} + \omega - is}\right] \tag{B.1}$$

* This appendix has been arranged while preparing Ref. 110. However, it has not been included into the final (revised) version of ref. [110].

Replacing the sum over **k** by an integral, this equation can be represented as

$$\theta_{lj}(\omega, \mathbf{R}) = (-\nabla^2 \delta_{lj} + \nabla_l \nabla_j) A(\omega, R) \tag{B.2}$$

with

$$A(\omega, R) = -\frac{1}{16\pi^3 c\varepsilon_0} \sum_m \int_0^\infty \mathrm{d}k \left(\frac{\omega_k^{(m)} v_g^{(m)}}{n(\omega_k^{(m)})} \right) \left[\frac{[n(\omega_k^{(m)})]^2 + 2}{3} \right]^2 \times \int \mathrm{d}\hat{\mathbf{k}} \left[\frac{e^{i\mathbf{k}.\mathbf{R}}}{\omega_k^{(m)} - \omega - is} + \frac{e^{-i\mathbf{k}.\mathbf{R}}}{\omega_k^{(m)} + \omega + is} \right] \tag{B.3}$$

where, for convenience, the sign of the infinitesimal s has been reversed in the nonresonant energy denominator. This does not alter the integral, since the frequency ω is considered to be a positive quantity. The angular integration may now be accomplished to yield

$$A(\omega, R) = \sum_m \int_0^\infty \mathrm{d}k \frac{\mathrm{d}\omega_k^{(m)}}{\mathrm{d}k} f(\omega_k^{(m)})(e^{-ikR} - e^{ikR}) \tag{B.4}$$

with

$$f(z) = \frac{1}{8\pi^2 i\varepsilon_0 R} \left[\frac{[n(z)]^2 + 2}{3n(z)} \right]^2 \left(\frac{1}{z - \omega - is} + \frac{1}{z + \omega + is} \right) \tag{B.5}$$

where we have utilized Eq. (3.14) for $\omega_k^{(m)}$, as well as the fact that $v_g^{(m)} = \mathrm{d}\omega_k^{(m)}/\mathrm{d}k$.

Substituting $z = \omega_k^{(m)}$, we find that Eq. (B.4) takes the form

$$A(\omega, R) = \int_C (e^{-izn(z)R/c} - e^{izn(z)R/c}) f(z) \mathrm{d}z \tag{B.6}$$

where summation over polariton bands $m = 1, 2, \ldots, M + 1$ has been accommodated by choosing the appropriate integration contour C (shown in Fig. 6*a*) that covers the real axis from 0 to $+\infty$, excluding the bandgap areas (see also Fig. 4). In other words, the contour C comprises segments restricted by the upper and lower boundaries of polariton bands, for which $n(z_+^{(m)}) = \infty$ and $n(z_-^{(m)}) = 0$, respectively.

Since $f(-z) = -f(z)$, the contour of integration may be expanded symmetrically to the negative values of z to yield

$$A(\omega, R) = \frac{1}{2} \int_{C_1} e^{-izn(z)R/c} f(z) \mathrm{d}z - \frac{1}{2} \int_{C_1} e^{izn(z)R/c} f(z) \mathrm{d}z \tag{B.7}$$

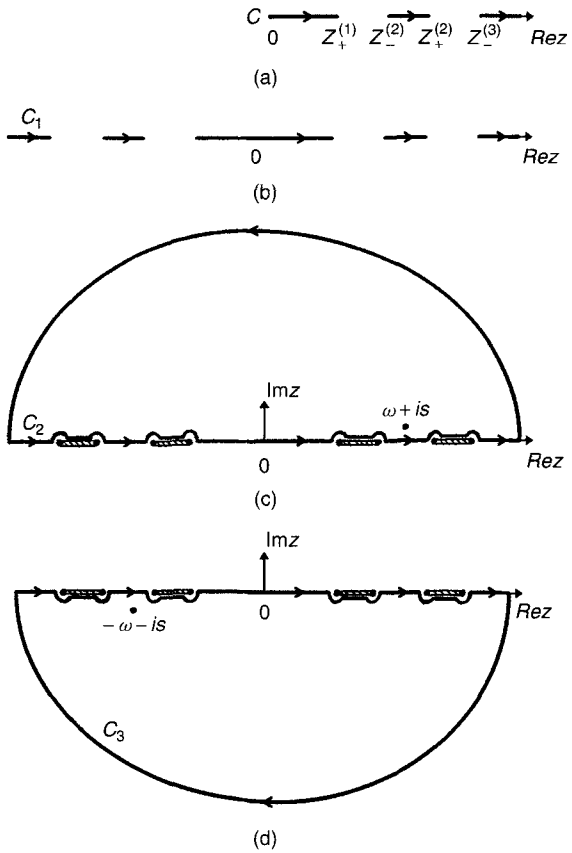

FIGURE 6. Contours of integration. (*a*) Integration contour C featured in Eq. (B.6). The contour comprises a number of solid lines representing a set of $M + 1$ polariton bands, where M is the number of molecular frequencies accommodated ($M = 2$ in the figure). The upper and lower boundaries of the individual bands are the branchpoints of the integral at $z = z_+^{(m)}$ and $z = z_-^{(m)}$, for which $n(z_+^{(m)}) = \infty$ and $n(z_-^{(m)}) = 0$, respectively. Arrows refer to the direction of integration. (*b*) Symmetric expansion of the original contour C to the negative values of z, producing the contour C_1. The branchpoints are extended symmetrically to the negative values of z as well. (*c*,*d*) Subsequent extension of the contour C_1 to either positive (*c*) or negative (*d*) imaginary half-planes, giving the new contours C_2 or C_3, respectively. The hatched lines are the branchcuts that connect the neighbouring branchpoints $z = \pm z_+^{(m-1)}$ and $z = \pm z_-^{(m)}$.

where the new contour C_1 is as shown in Fig. 6*b*. To convert the integration contour C_1 into the closed one, we choose the branchcuts connecting the neighboring branchpoints $z = \pm z_+^{(m-1)}$ and $z = \pm z_-^{(m)}$. The contour may then be extended over either upper or lower imaginary half-planes to include the bandgap areas, subsequently closing it up with a large semicircle, as

demonstrated in Fig. 6*c*, *d*. The resulting contours C_2 and C_3 will apply, respectively, to the first and second terms of Eq. (B.7), giving

$$A(\omega, R) = \frac{1}{2}\oint_{C_2} e^{-izn(z)R/c} f(z)\mathrm{d}z - \frac{1}{2}\oint_{C_3} e^{izn(z)R/c} f(z)\mathrm{d}z \tag{B.8}$$

The extension of the integration contours does not alter the value of the integral. Integrals over the large semicircles go to the zero, as the integration radius goes to the infinity. Next, the sign of the refractive index $n(z) \equiv \sqrt{\varepsilon(z)}$ is opposite at the opposite edges of the branchcuts, so that both terms of Eq. (B.8) cancel each other, performing an extra integration the over the bandgap areas. Finally, the integrals over the (infinitely) small semicircles around the branchpoints are mutually canceled in an obvious way as well.

The residuum theorem may now be applied. Calculating residues at $z = \pm\omega \pm is$, one finds

$$A(\omega, R) = -\frac{1}{4\pi\varepsilon_0 n^2}\left[\frac{n^2+2}{3}\right]^2 \frac{e^{i\omega nR/c}}{R} \tag{B.9}$$

where the refractive index n [defined by Eqs. (3.15) and (3.16)] is to be calculated at the frequency $\omega + is$ containing a small imaginary part, as expressed by Eq. (3.19). In an absorbing region, the molecular frequencies Ω_γ form a quasicontinuum of vibrational, rotational, or other sublevels. The integration contour contains then a densely spaced set of tiny bandlines that reduces to a quasicontinuum of quasidots, as the spacing between the frequencies Ω_γ goes to zero. Under this condition, retention of the infinitesimal $s \to +0$ plays an important role in the subsequent procedure of smoothing of the quasidiscrete molecular spectrum. In such a procedure, the quantity s is considered to be larger than a characteristic distance of separation between the molecular frequencies Ω_γ. As a result, a finite imaginary part in'' appears in the refractive index (3.19).

Finally, calling on Eqs. (B.2) and (B.9), one arrives to required result (3.18) for the tensor $\theta_{lj}(\omega, \mathbf{R})$. Note that the branch-dependent group velocity $v_{\mathrm{g}}^{(m)} = \mathrm{d}\omega_k^{(m)}/\mathrm{d}k$ no longer features in the final result for $\theta_{ij}(\omega, \mathbf{R})$, since it has been canceled by making a substitution $z = \omega_k^{(m)}$ in Eq. (B.6).

ACKNOWLEDGMENTS

The authors wish to thank T. Thirunamachandran for helpful discussions, as well as P. Allcock and A. Kuliešas for their assistance in preparing some of the figures.

REFERENCES

1. E. Fermi, *Rep. Mod. Phys.* **4**, 87–132 (1932).
2. W. Heitler and S. T. Ma, *Proc. Roy. Irish Acad.* **52**, (Sect. A), 109–125 (1949).
3. J. Hamilton, *Proc. Phys. Soc. (London)* **62**, 12–18 (1949).
4. S. Kikuchi, *Z. Phys.* **66**, 558–571 (1930).
5. B. J. Birks, *The Theory and Practice of Scintillation Counting*, Pergamon Press, Oxford, 1964.
6. M. D. Galanin, *Luminescence of Molecules and Crystals*, Cambridge International Scientific Publishers, Cambridge, UK, 1996.
7. F. Perrin, *Ann. Phys. (Paris)* **17**, 283–314 (1932).
8. Th. Förster, *Ann. Physik* **6**, 55–75 (1948).
9. D. L. Dexter, *J. Chem. Phys.* **21**, 836–850 (1953).
10. M. D. Galanin, *Zh. Eksp. Theoret. Fiz.* **28**, 485–495. (1953).
11. V. M. Agranovich and M. D. Galanin, *Electronic Excitation Energy Transfer in Condensed Matter*, North-Holland, Amsterdam, 1982.
12. S. Gnanakaran, G. Haran, R. Kumble, and R. M. Hochstrasser, in *Resonance Energy Transfer*, D. L. Andrews and A. A. Demidov, eds., Wiley, New York, 1999, pp. 308–365.
13. R. Van Grondelle and O. J. G. Somsen, in *Resonance Energy Transfer*, D. L. Andrews and A. A. Demidov, eds., Wiley, New York, 1999, pp. 366–398.
14. S. Savikhin, D. R. Buck, and W. S. Struve, in *Resonance Energy Transfer*, D. L. Andrews and A. A. Demidov, eds., Wiley, New York, 1999, pp. 399–434.
15. J. S. Avery, *Proc. Phys. Soc. (London)* **88**, 1–8 (1966).
16. L. Gomberoff and E. A. Power, *Proc. Phys. Soc. (London)* **88**, 281–284 (1966).
17. E. A. Power and T. Thirunamachandran, *Phys. Rev. A* **28**, 2671–2675 (1983).
18. J. S. Avery, *Int. J. Quant. Chem.* **25**, 79–96 (1984).
19. D. L. Andrews and B. S. Sherborne, *J. Chem. Phys.* **86**, 4011–4017 (1987).
20. D. L. Andrews, D. P. Craig, and T. Thirunamachandran, *Int. Rev. Phys. Chem.* **8**, 339–383 (1989).
21. D. L. Andrews, *Chem. Phys.* **135**, 195–201 (1989).
22. D. P. Craig and T. Thirunamachandran, *Chem. Phys.* **135**, 37–48 (1989).
23. D. L. Andrews and G. Juzeliūnas, *J. Chem. Phys.* **95**, 5513–5518 (1991).
24. D. L. Andrews and G. Juzeliūnas, *J. Chem. Phys.* **96**, 6606–6612 (1992).
25. D. P. Craig and T. Thirunamachandran, *Chem. Phys.* **167**, 229–240 (1992).
26. G. D. Scholes, A. H. A. Clayton, and K. P. Ghiggino, *J. Chem. Phys.* **97**, 7405–7413 (1992).
27. G. Juzeliūnas and D. L. Andrews, *Phys. Rev. B* **49**, 8751–8763 (1994).
28. G. Juzeliūnas and D. L. Andrews, *Phys. Rev. B* **50**, 13371–13378 (1994).
29. M. N. Berberan-Santos, E. J. Nunes Pereira, and J. M. G. Martinho, *J. Chem. Phys.* **103**, 3022–3028 (1995).
30. G. D. Scholes and D. L. Andrews, *J. Chem. Phys.* **107**, 5374–5384 (1997).
31. G. Juzeliūnas, *Phys. Rev. A* **55**, R4015–R4018 (1997).

32. R. D. Jenkins and D. L. Andrews, *J. Phys. Chem. A* **102**, 10834–10842 (1998).
33. G. D. Scholes and K. P. Ghiggino, *J. Phys. Chem.* **98**, 4580–4590 (1994).
34. D. A. Hutchinson and H. F. Hameka, *J. Chem. Phys.* **41**, 2006–2011 (1964).
35. M. J. Stephen, *J. Chem. Phys.* **40**, 669–673 (1964).
36. P. W. Milonni and P. L. Knight, *Phys. Rev. A* **10**, 1096–1108 (1974).
37. A. A. Serikov and Yu. M. Khomenko, 1978. *Physica* **93C**, 383–392 (1978).
38. D. Kaup and V. I. Rupasov, *J. Phys. A: Math. Gen.* **29**, 6911–6923 (1996).
39. M. I. Shirokov, *Yad. Fiz.* **4**, 1077 [*Sov. J. Nucl. Phys.* **4**, 774 (1967)]; *Usp. Fiz. Nauk* **124**, 697–715 (1978) [*Sov. Phys. Usp.* **21**, 345 (1978)].
40. B. Ferretti, in *Old and New Problems in Elementary Particles*, G. Puppi, ed., Academic, Press, New York, 1968, p. 108.
41. G. C. Hegerfeldt, *Phys. Rev. D* **10**, 3320 (1974).
42. V. P. Bykov and A. A. Zadernovsky, *Zh. Exp. Theoret. Phys.* **81**, 37–45 (1981).
43. M. H. Rubin, *Phys. Rev. D* **35**, 3836–3839 (1987).
44. A. K. Biswas, G. Compagno, R. Passante, and F. Persico, *Phys. Rev. A* **42**, 4291–4301 (1990).
45. A. Valentini, *Phys. Lett. A* **153**, 321–325 (1991).
46. G. C. Hegerfeldt, *Phys. Rev. Lett.* **72**, 596–599 (1994).
47. D. Buchholz and J. Yngvason, *Phys. Rev. Lett.* **73**, 613–616 (1994).
48. G. Compagno, G. M. Palma, R. Passante, and F. Persico, *Chem. Phys.* **198**, 19–23 (1995).
49. P. W. Milonni, D. F. V. James, and H. Fearn, *Phys. Rev. A* **52**, 1525–1537 (1995).
50. E. A. Power and T. Thirunamachandran, 1997. *Phys. Rev. A* **56**, 3395–3408 (1997).
51. P. R. Berman and B. Dubetsky, *Phys. Rev. A* **55**, 4060–4069 (1997).
52. G. C. Hegerfeldt, *Ann. Phys.* **7**, 716–725 (1998).
53. R. H. Lehmberg, *Phys. Rev. A* **2**, 889–896 (1970).
54. G. S. Agarwal, in relation to other approaches. *In Springer Tracts in Modern Physics*, G. Höhler, ed., Springer-Verlag, Berlin, Vol. 70, p. 64.
55. Z. Ficek, R. Tanas, and S. Kielich, *Optica Acta* **33**, 1149–1160 (1986).
56. D. F. James, *Phys. Rev. A* **47**, 1336–1346 (1993).
57. R. G. Brewer, *Phys. Rev. A* **52**, 2965–2970 (1995); *Phys. Rev. Lett.* **77**, 5153–5156 (1996).
58. R. G. De Voe and R. G. Brewer, *Phys. Rev. Lett.* **76**, 2049–2052 (1996).
59. J. Guo and J. Cooper, 1995. *Phys. Rev. A* **51**, 3128–3135 (1995).
60. A. W. Vogt, J. I. Cirac, and P. Zoller, *Phys. Rev. A* **53**, 950–968 (1996).
61. H. Morawitz, *Phys. Rev.* **187**, 1792–1796 (1969).
62. J. Kuhn, *Chem. Phys.* **53**, 101–108 (1970).
63. K. H. Drexhage, *J. Lumin.* **1/2**, 693–701 (1970).
64. H. Morawitz and M. R. Philpott, 1974. *Phys. Rev. B* **10**, 4863–4868 (1974).
65. R. R. Chance, A. Prock, and R. Silbey, in *Advances in Chemical Physics*, I. Prigogine and S. A. Rice, eds., Wiley, New York, 1978, Vol. 37, p. 1.
66. G. Juzeliūnas and D. L. Andrews, *Chem. Phys.* **200**, 3–10 (1995).
67. D. L. Andrews and P. Allcock, *Chem. Soc. Rev.* **24**, 259–265 (1995).
68. E. Hudis, Y. Ben-Aryeh, and U.P. Oppenheim, *Phys. Rev. A* **43**, 3631–3639 (1991).
69. D. L. Andrews and P. Allcock, 1994. *Chem. Phys. Lett.* **231**, 206–210 (1994).

70. G. Kweon and N. M. Lawandy, *Phys. Rev. B* **49**, 4445–4454 (1994).
71. S. John and J. Wang, *Phys. Rev. B* **43**, 12772–12789 (1991).
72. J. Knoester and S. Mukamel, *Phys. Rev. A* **40**, 7065–7080 (1989).
73. G. Juzeliūnas, *J. Lumine.* **76/77**, 666–669 (1998).
74. G. Kurizki and A. Z. Genack, *Phys. Rev. Lett.* **61**, 2269–2271 (1988).
75. G. Kurizki, *Phys. Rev. A* **42**, 2915–2924 (1990).
76. G.-I. Kweon and N. M. Lawandy, *J. Mod. Opt.* **41**, 311–323 (1994).
77. S. Bay, P. Lambropoulos, and K. Molmer, *Phys. Rev. A* **55**, 1485–1496 (1997).
78. V. I. Rupasov and M. Singh, *Phys. Rev. A* **56**, 898–904 (1997).
79. Q. Zheng, T. Kobayashi, and T. Sekiguchi, *Phys. Rev. Lett.* **77**, 406 (1996).
80. T. Kobayashi, Q. Zheng, and T. Sekiguchi, *Phys. Rev. A* **52**, 2835–2846 (1995).
81. M. Hopmeier, W. Guss, M. Deussen, E. O. Göbel, and R. F. Mahrt, *Phys. Rev. Lett.* **82**, 4118–4121 (1999).
82. S. Druger, S. Arnold, and L. M. Folan, *J. Chem. Phys.* **87**, 2649–2659 (1987).
83. P. T. Leung and K. Young, *J. Chem. Phys.* **89**, 2894–2899 (1988).
84. M. Tomita, K. Ohosumi, and H. Ikari, *Phys. Rev. B* **50**, 10369–10372 (1994).
85. M. Cho and R. Silbey, *Chem. Phys. Lett.* **242**, 291–296 (1995).
86. V. V. Klimov and V. S. Letokhov, *Phys. Rev. A* **58**, 3235–3247 (1998).
87. G. Kurizki, A. G. Kofman, and V. Yudson, *Phys. Rev. A* **53**, R35–R38 (1996).
88. E. V. Goldstein and P. Meystre, *Phys. Rev. A* **56**, 5135–5146 (1997).
89. E. Yablonovich, *Phys. Rev. Lett.* **58**, 2059–2062 (1987).
90. E. Yablonovich, T. J. Gmitter, and R. Batt, *Phys. Rev. Lett.* **61**, 2546–2549 (1988).
91. J. P. Dowling and C. M. Bowden, *Phys. Rev. A* **46**, 612–622 (1992).
92. S. John and T. Quang, *Phys. Rev. A* **50**, 1764–1769 (1994).
93. A. Kaufman, G. Kurizki, and B. Sherman, *J. Mod. Opt.* **41**, 353–384 (1994).
94. E. A. Power, *Introductory Quantum Electrodynamics*, Longmans, London, 1964.
95. W. P. Healy, *Non-relativistic Quantum Electrodynamics*, Academic Press, London, 1982.
96. D. P. Craig and T. Thirunamachandran, *Molecular Quantum Electrodynamics*. Academic press, New York, 1984.
97. E. A. Power and S. Zienau, *Philos. Trans. Roy. Soc. London A* **251**, 427–454 (1959).
98. R. G. Woolley, *Proc. Roy. Soc. London A* **321**, 557–572. (1971).
99. P. W. Milonni, *The quantum Vacuum: An Introduction to Quantum Electrodynamics*, Academic press, San Diego, 1994.
100. P. Meystre, *Phys. Rev. A* **53**, 3573–3581 (1996).
101. P. Allcock, R. D. Jenkins, and D. L. Andrews, *Chem. Phys. Lett.* **301**, 228–234 (1999).
102. L. S. Rodberg and R. M. Thaler, *Introduction to the Quantum Theory of Scattering*. Academic press, New York, 1967. Chapter 8.
103. G. Kurizki and J. W. Haus, eds., 1994, *Photonic Band Structures*, *J. Mod. Opt.* **41** (2) (special issue) (1994).
104. S. John and J. Wang, *Phys. Rev. Letts.* **64**, 2418–2421. (1990).
105. G. Juzeliūnas and A. Kuliešas, in press.
106. M. Lewenstein, J. Zakrzewski, T. W. Mossberg, and J. Mostowski, *J. Phys. B—Atom. Mol. Opt. Phys.* **21**, L9–L14. (1988).

107. M. Lewenstein, J. Zakrzewski, and T. W. Mossberg, *Phys. Rev. A* **38**, 808–819 (1988).
108. H. Giessen, J. D. Berger, G. Mohs, P. Meystre, and S. F. Yelin, *Phys. Rev. A* **53**, 2816–2821 (1996).
109. G. Juzeliūnas, *Chem. Phys.* **198**, 145–158 (1995).
110. G. Juzeliūnas, *Phys. Rev. A* **53**, 3543–3558 (1996).
111. G. Juzeliūnas, *Phys. Rev. A* **55**, 929–934 (1997).
112. P. De Vries and A. Lagendijk, *Phys. Rev. Lett.* **81**, 1381–1384 (1998).
113. P. D. Drummond and M. Hillery, *Phys. Rev. A* **59**, 691–707 (1999).
114. J. C. Slater, *Electronic Structure of Molecules*, McGraw-Hill, New York, 1963, Chapter 1.
115. B. V. Van der Meer, *Resonance Energy Transfer*, D. L. Andrews and A. A. Demidov, eds., Wiley, New York, 1999, pp. 151–172.
116. R. E. Dale and J. Eisinger, *Biopolymers* **13**, 1573 (1974).
117. P. Allcock and D. L. Andrews, *J. Chem. Phys.* **108**, 3089–3095 (1998).
118. H. Khosravi and R. Loudon, *Proc. Roy. Soc. London. A* **436**, 373–389 (1992).
119. O. N. Godomsky and K. V. Krutitsky, *Zh. Exp. Theoret. Phys.* **106**, 936–955 (1994).
120. M. S. Yeung and T. K. Gustafson, *Phys. Rev. A* **54**, 5227–5242 (1996).
121. H. P. Urbach and G. L. J. A. Rikken, *Phys. Rev. A* **57**, 3913–3930 (1998).
122. R. J. Glauber and M. Lewenstein, *Phys. Rev. A* **43**, 467–491 (1991).
123. S. M. Barnett, B. Huttner, and R. Loudon, *Phys. Rev. Lett.* **68**, 3698–3701 (1992).
124. S. M. Barnett, B. Huttner, R. Loudon, and R. Matloob, *J. Phys. B—Atom. Mol. Opt. Phys.* **29**, 3763–3781 (1996).
125. S. T. Ho and P. Kumar, *J. Opt. Soc. Am. B* **10**, 1620–1636 (1993).
126. P. W. Milonni, *J. Mod. Opt.* **42**, 1991–2004 (1995).
127. G. L. J. A. Rikken and Y. A. R. R. Kessener, *Phys. Rev. Lett.* **74**, 880–883 (1995).
128. F. J. P. Schuurnams, D. T. N. de Lang, G. H. Wegdam, R. Sprik, and A. Lagendijk, *Phys. Rev. Lett.* **80**, 5077–5080 (1988).
129. A. R. Von Hippel, *Dielectrics and Waves*, Wiley, New York, 1954, Section I.13.
130. J. A. Wheeler and R. P. Feynman, *Rev Mod. Phys.* **21**, 425–433 (1949).
131. D. T. Pegg, *Ann. Phys. (NY)* **118**, 1–17 (1979).
132. A. V. Durrant, *Proc. Roy. Soc. Lond. A* **370**, 41–59 (1980).
133. W. Heitler, *The Quantum Theory of Radiation*, Oxford Univ. Press, New York, 1954, p. 163.
134. G. Juzeliūnas and D. L. Andrews, in *Resonance Energy Transfer*, D. L. Andrews and A. A. Demidov, eds., Wiley, New York, 1999, p. 65–107.
135. E. A. Power and T. Thirunamachandran, *Chem. Phys.* 171: 1–7 (1993).
136. J. D. Jackson, *Classical Electrodynamics*, Wiley, New York, 1962, Section 4.6.
137. M. Orrit and P. Kottis, in *Advances in Chemical Physics*, I. Prigogine and S. A. Rice, eds., Wiley, New York, 1988, Vol. 74, p. 1.